SNUTP-94-50
hep-ph/9406311
June 1994



# An Effective Chiral Lagrangian Approach to Kaon-Nuclear Interactions:

## *Kaonic atom and kaon condensation*

Chang-Hwan Lee[a], G. E. Brown[b], Dong-Pil Min[a] and Mannque Rho[c]
a) *Department of Physics and Center for Theoretical Physics, Seoul National University, Seoul 151-742, Korea*
b) *Department of Physics, State University of New York, Stony Brook, N.Y. 11794, USA.*
c) *Service de Physique Théorique, CEA Saclay 91191 Gif-sur-Yvette Cedex, France*

**ABSTRACT**

On-shell kaon-nucleon scattering, kaonic atom and kaon condensation are treated on the same footing by means of a chiral perturbation expansion to the next-to-next-to-leading order ("N$^2$LO"). Constraining the low-energy constants in the chiral Lagrangian by on-shell $KN$ scattering lengths and kaonic atom data, the off-shell s-wave scattering amplitude up to one-loop order corresponding to N$^2$LO and the critical density of kaon condensation up to *in-medium* two-loop order are computed. The effects on kaon-proton scattering of the quasi-bound $\Lambda(1405)$ and on kaonic atoms and kaon condensation of $\Lambda(1405)$-proton-hole excitations through four-Fermi interactions are studied to all orders in density within the *in-medium* two-loop approximation. It is found that the four-Fermi interaction terms in the chiral Lagrangian play an essential role in providing attraction for kaonic atoms, thereby inducing condensation but the critical density is remarkably insensitive to the strength of the four-Fermi interaction that figures in kaonic atoms. The prediction for the critical density is extremely robust and gives – for "natural" values of the four-Fermi interactions – a rather low critical density, $\rho_c \lesssim 4\rho_0$. When the BR scaling is suitably implemented, the condensation sets in at $\rho_c \simeq 2\,\rho_0$ with loop corrections and four-Fermi interactions playing a minor role.

# 1 Introduction

In a series of recent short papers[1, 2, 3], we have discussed kaon-nucleon and kaon-nuclear interactions in terms of a chiral perturbation expansion with the objective to predict within the framework of chiral effective Lagrangians the onset of kaon condensation in dense hadronic matter relevant to compact stars that are formed from the gravitational collapse of massive stars. This research was given a stronger impetus by a recent suggestion of Brown and Bethe [4] that if kaon condensates develop at a matter density $\rho \lesssim 4\ \rho_0$ (where $\rho_0 \approx 0.16/fm^3$ is normal nuclear matter density) in the collapse of large stars, then low-mass black holes are highly likely to form in place of neutron stars of the mass greater than 1.5 times the solar mass $M_\odot$. The purpose of this paper is to provide the details of our previous publications, such as the approximations made, inherent uncertainties involved etc. with complete and explicit formulae that we were unable to supply in the letter papers because of the space limitation. In addition, some additional justifications that have in the meantime been uncovered and understood better will be discussed.

Ever since the first paper of Kaplan and Nelson[5], there have been numerous investigations on kaon condensation in dense neutron-star matter as well as in nuclear matter based both on effective chiral Lagrangians[1, 6, 7, 8, 9] and on phenomenological off-shell meson-nucleon interactions[10, 11]. The two ways of addressing the problem gave conflicting results with the chiral Lagrangian approaches generally predicting a relatively low critical density, $\rho_c \sim (2-4)\rho_0$, while the phenomenological approaches based more or less on experimental inputs giving results that tend to exclude condensation at a low enough density to make it relevant in the collapse process.

We should stress that it is not our purpose here to clarify what makes the phenomenological approach differ from the chiral Lagrangian approach. Instead, our objective in this paper is to do as consistent and systematic a calculation as possible in the context of chiral perturbation theory. This effort is largely motivated from the strong-interaction point of view by the recent success in confronting, in terms of chiral dynamics, the classic nuclear physics problems such as nuclear forces[12, 13] and exchange currents[14, 15, 16]. This paper addresses the problem of applying chiral perturbation theory to multi-hadron systems that contain the strange-quark flavor. While the standard problems of nuclear physics such as nuclear forces and exchange currents involve the chiral quarks $u$ and $d$ for which the mass scale involved is small compared with the typical QCD chiral symmetry breaking scale $\Lambda_\chi \sim 1$ GeV so that a simultaneous expansion in derivatives and quark mass matrix is justified, here the strange-quark mass which is not small renders the expansion in the quark mass a lot more delicate and hence the low-order expansion highly problematic. This caveat has to be kept in mind in assessing the validity of the procedure we will adopt.

Another problem of potential importance is that both kaonic atom and kaon condensation introduce an additional scale, namely the matter density $\rho$ or more precisely the Fermi momentum $k_F$. So far in low-order chiral perturbation calculations, the result depended on the order of density dependence included in the calculation. In fact, one of the important differences between the chiral Lagrangian approach and the phenomenological model approach arose at the order $\rho^2$. It is thus clear that one has to be consistent in the chiral counting, not only with respect to the usual expansion parameters practiced in free space, but also with respect to the density expansion. This then raises the question of how to treat the dynamics involved in the non-strange sector as well as in the strange sector. So far the dynamics in the non-strange sector is assumed to be given by what we know from nuclear phenomenology that is mostly given in terms of meson-theoretic

approaches combined with many-body techniques, and perturbations in the strange direction are treated in terms of chiral Lagrangian at tree order or at most one-loop order. The problem with this is that there is no consistency between the two sectors as regards chiral symmetry and other constraints of QCD. Indeed so far nobody has been able to describe correctly nuclear ground state (including nuclear matter) starting from chiral Lagrangians, so one is justified to wonder how a low-order chiral Lagrangian calculation of kaon condensation without regard to the normal matter can be trusted. We cannot offer a solution to this problem here but we will make an effort to point out the salient points that are closely related to this issue.

Following the recent development of nuclear chiral dynamics [12, 13, 14, 15, 16], we incorporate spontaneously broken chiral symmetry using the Jenkins-Manohar heavy-baryon chiral Lagrangian [17] as extended in [2] to $\mathcal{O}(Q^3)$ to describe s-wave kaon nucleon scattering to one loop order in chiral perturbation theory (ChPT). In addition to the usual octet and decuplet baryons and the octet pseudo-Goldstone fields, the $\Lambda(1405)$ was found to figure importantly in the kaon-nucleon process. This is because as is well-known, the $\Lambda(1405)$ (which we denote $\Lambda^\star$ for short) influences strongly the amplitude of the $K^-p$ scattering near threshold and hence kaon-nuclear interactions in kaonic atom [18] and kaon condensation involving protons as in "nuclear stars." We introduce this state as an elementary field as discussed in [2]. The reason for this is that first of all, the $\Lambda^\star$ is a bound state and hence cannot be described by a finite chiral perturbation expansion and secondly in the Callan-Klebanov skyrmion description [19], it is a configuration of a $K^-$ wrapped by an $SU(2)$ soliton and hence is as "elementary" as the even-parity $\Lambda(1115)$ of the octet baryon.

In addition to these terms operating in the single-baryon sector, we need terms that involve multi-baryon fields in the Lagrangian for describing many-body systems. There have been discussions of four-Fermi interaction terms in non-strange sectors [12, 13, 15, 20]. We find that in the s-wave kaon-nuclear sector, two such four-Fermi interaction terms involving $\Lambda^\star$ can intervene. In p-wave kaon-nuclear interactions, there can be more four-Fermi interactions as they can involve the entire battery of the octet and decuplet but we will not be concerned with them in this paper.

By a straightforward extension of an amplitude whose parameters are fixed by on-shell kaon-nucleon scattering, we are able to almost (but not quite) uniquely predict an off-shell kaon-nucleon amplitude relevant for kaonic-atom as well as kaon-condensation phenomena. The predicted off-shell amplitude was found to be in fair agreement with the phenomenological fit [21]. This off-shell amplitude provides the kaon self-energy in linear density approximation, equivalent to the usual optical potential approximation. The critical density obtained in this approximation is a bit higher than that obtained before at tree order but still in the regime quite relevant to the stellar collapse. If one goes beyond the linear density approximation which would be required in a simultaneous expansion in all the scales involved, four-Fermion interactions come into play. For the s-wave kaon condensation process, there are two independent four-Fermi interactions with arbitrary constants. In order to fix these parameters, we appeal to the recent data on kaonic atoms[18]. We are able to fix unambiguously only one of the two constants with the presently available data. While the other constant remains free, its sign and magnitude can, however, be constrained by a "naturalness" condition and furthermore the physical quantities that we are interested in turn out to be rather insensitive to the free parameter.

The four-Fermi interactions – which are higher order in density – play an important role for giving rise to an attraction for kaonic atoms. This attraction certainly comes in for *pushing* the

system toward condensation. However, they remain "irrelevant" and become suppressed at the kinematic regime in which condensation occurs. As a consequence, their influence on the critical density is quite weak: The strength of the four-Fermi interactions, which cannot be pinned down precisely at present, does not figure importantly in the condensation phenomena.

We do not consider six-Fermi and higher-Fermi interactions as they would be further suppressed by the scale set by the chiral symmetry breaking scale $\Lambda_\chi \sim 1$ GeV.

The paper is organized as follows. The effective chiral Lagrangian to $\mathcal{O}(Q^3)$ in the chiral counting, consisting of the octet pseudo-Goldstone bosons and the octet and decuplet baryons that figure in our calculation, is given in section 2. In section 3, we calculate to one-loop order, corresponding to N$^2$LO, both on-shell and off-shell KN scattering amplitudes. Some issues regarding Adler's soft-meson conditions in chiral perturbation theory are also discussed. Kaonic atom is treated in section 4 and kaon condensation in sections 5 and 6. In section 7, we mention some of the unsolved open issues in the problem. Detailed formulas are collected in the appendices.

## 2 Effective Chiral Lagrangian

We start by writing down the effective chiral Lagrangian that we shall use in the calculation. Let the characteristic momentum/energy scale that we are interested in be denoted $Q$. The standard chiral counting orders the physical amplitude as a power series in $Q$, say, $Q^\nu$, with $\nu$ an integer. To leading order, the kaon-nucleon amplitude $T^{KN}$ goes as $\mathcal{O}(Q^1)$, to next order as $\mathcal{O}(Q^2)$ involving no loops and to next to next order (*i.e.*, N$^2$LO) at which one-loop graphs enter as $\mathcal{O}(Q^3)$. Following Jenkins and Manohar [17], we denote the velocity-dependent octet baryon fields $B_v$, the octet meson fields $\exp(i\pi_a T_a/f) \equiv \xi$, the velocity-dependent decuplet baryon fields $T_v^\mu$, the velocity four-vector $v_\mu$ and the spin operator $S_v^\mu$ ($v\cdot S_v = 0$, $S_v^2 = -3/4$), the vector current $V_\mu = [\xi^\dagger, \partial_\mu \xi]/2$ and the axial-vector current $A_\mu = i\{\xi^\dagger, \partial_\mu \xi\}/2$, and write the Lagrangian density to order $Q^3$, relevant for the low-energy s-wave scattering[#1], as

$$
\begin{aligned}
\mathcal{L}^{(1)} &= \mathrm{Tr}\ \bar{B}_v (iv\cdot\mathcal{D}) B_v + 2D\mathrm{Tr}\ \bar{B}_v S_v^\mu \{A_\mu, B_v\} + 2F\mathrm{Tr}\ \bar{B}_v S_v^\mu [A_\mu, B_v] \\
&\quad -\bar{T}_v^\mu (iv\cdot\mathcal{D} - \delta_T) T_{v,\mu} + \mathcal{C}(\bar{T}_v^\mu A_\mu B_v + \bar{B}_v A_\mu T_v^\mu) + 2\mathcal{H}\bar{T}_v^\mu (S_v\cdot A) T_{v,\mu} \qquad (1) \\
\mathcal{L}^{(2)} &= a_1 \mathrm{Tr}\ \bar{B}_v \chi_+ B_v + a_2 \mathrm{Tr}\ \bar{B}_v B_v \chi_+ + a_3 \mathrm{Tr}\ \bar{B}_v B_v \mathrm{Tr}\ \chi_+ \\
&\quad + d_1 \mathrm{Tr}\ \bar{B}_v A^2 B_v + d_2 \mathrm{Tr}\ \bar{B}_v (v\cdot A)^2 B_v + d_3 \mathrm{Tr}\ \bar{B}_v B_v A^2 + d_4 \mathrm{Tr}\ \bar{B}_v B_v (v\cdot A)^2 \\
&\quad + d_5 \mathrm{Tr}\ \bar{B}_v B_v \mathrm{Tr}\ A^2 + d_6 \mathrm{Tr}\ \bar{B}_v B_v \mathrm{Tr}\ (v\cdot A)^2 + d_7 \mathrm{Tr}\ \bar{B}_v A_\mu\ \mathrm{Tr}\ B_v A^\mu \\
&\quad + d_8 \mathrm{Tr}\ \bar{B}_v (v\cdot A)\ \mathrm{Tr}\ B_v (v\cdot A), \qquad (2) \\
\mathcal{L}^{(3)} &= c_1 \mathrm{Tr}\ \bar{B}_v (iv\cdot\mathcal{D})^3 B_v + g_1 \mathrm{Tr}\ \bar{B}_v A_\mu (iv\cdot \overleftrightarrow{\mathcal{D}}) A^\mu B_v + g_2 \mathrm{Tr}\ B_v A_\mu (iv\cdot \overleftrightarrow{\mathcal{D}}) A^\mu \bar{B}_v \\
&\quad + g_3 \mathrm{Tr}\ \bar{B}_v v\cdot A (iv\cdot \overleftrightarrow{\mathcal{D}}) v\cdot A B_v + g_4 \mathrm{Tr}\ B_v v\cdot A (iv\cdot \overleftrightarrow{\mathcal{D}}) v\cdot A \bar{B}_v \\
&\quad + g_5 \left( \mathrm{Tr}\ \bar{B}_v A_\mu \mathrm{Tr}\ (iv\cdot \overrightarrow{\mathcal{D}}) A^\mu B_v - \mathrm{Tr}\ \bar{B}_v A_\mu (iv\cdot \overleftarrow{\mathcal{D}}) \mathrm{Tr}\ A^\mu B_v \right) \\
&\quad + g_6 \left( \mathrm{Tr}\ \bar{B}_v v\cdot A \mathrm{Tr}\ B_v (iv\cdot \overrightarrow{\mathcal{D}}) v\cdot A - \mathrm{Tr}\ \bar{B}_v v\cdot A (iv\cdot \overleftarrow{\mathcal{D}}) v\cdot A \mathrm{Tr}\ B_v v\cdot A \right) \\
&\quad + g_7 \mathrm{Tr}\ \bar{B}_v [v\cdot A, [iD^\mu, A_\mu]] B_v + g_8 \mathrm{Tr}\ B_v [v\cdot A, [iD^\mu, A_\mu]] \bar{B}_v \\
&\quad + h_1 \mathrm{Tr}\ \bar{B}_v \chi_+ (iv\cdot\mathcal{D}) B_v + h_2 \mathrm{Tr}\ \bar{B}_v (iv\cdot\mathcal{D}) B_v \chi_+ + h_3 \mathrm{Tr}\ \bar{B}_v (iv\cdot\mathcal{D}) B_v \mathrm{Tr}\ \chi_+
\end{aligned}
$$

[#1] The relevant terms in component fields useful for calculating Feynman diagrams are given in Appendix A.

$$+l_1 \mathrm{Tr}\ \bar{B}_v[\chi_-, v\cdot A]B_v + l_2 \mathrm{Tr}\ \bar{B}_v B_v[\chi_-, v\cdot A] + l_3[\mathrm{Tr}\ \bar{B}_v\chi_-, \mathrm{Tr}\ B_v v\cdot A], \tag{3}$$

where the covariant derivative $\mathcal{D}_\mu$ for baryon fields is defined by

$$\begin{aligned} \mathcal{D}_\mu B_v &= \partial_\mu B_v + [V_\mu, B_v], \\ \mathcal{D}_\mu T^\nu_{v,abc} &= \partial_\mu T^\nu_{v,abc} + (V_\mu)^d_a T^\nu_{v,dbc} + (V_\mu)^d_b T^\nu_{v,adc} + (V_\mu)^d_c T^\nu_{v,abd}, \end{aligned} \tag{4}$$

$\delta_T$ is the $SU(3)$ invariant decuplet-octet mass difference, and

$$\chi_\pm \equiv \xi\mathcal{M}\xi \pm \xi^\dagger\mathcal{M}\xi^\dagger, \tag{5}$$

with $\mathcal{M} = \mathrm{diag}\,(m_u, m_d, m_s)$ the quark mass matrix that breaks chiral symmetry explicitly. There are many other terms involving the decuplet that one can write down but we have written only those that enter in the calculation. Among the many parameters that figure in the Lagrangian, a few can be fixed right away. For instance, we will simply fix the constants $F$ and $D$ at tree order since to $\mathcal{O}(Q^3)$ that we will be interested in, they are not modified. We shall use $D = 0.81$ and $F = 0.44$. The constant $C$ can also be fixed at this stage from the decay process $\Delta(1230) \to N\pi$. We shall use $|C|^2 (\approx 2.58)$. Of course, the flavor $SU(3)$ can be substantially broken as we will discuss later, so one cannot take this value too seriously. The determination of all other constants $a_i$,..., $l_i$ (or more precisely the combinations thereof) will be described below.

The number of parameters that seem to enter may appear daunting to some readers but the situation turns out to be much simpler than what it looks. As we will see later, once the constants are grouped into an appropriate form, there remain only four parameters for on-shell $K^\pm N$ amplitudes. These parameters can be fixed on-shell by the four s-wave scattering lengths. Off-shell, however, one parameter remains free but the off-shell amplitude turns out to be rather insensitive to the one free parameter. This drastic simplification can be understood easily as follows. First of all, the heavy-fermion formalism (in short HFF) makes those subleading terms (*i.e.*, terms with $\nu \geq 2$) involving the spin operator $S_\mu$ vanish, since they are proportional to $S\cdot q$, $S\cdot q'$, or $S\cdot qS\cdot q'$, all of which are identically zero. As a consequence, there are no contributions to the $s$-wave meson-nucleon scattering amplitude from one-loop diagrams in which the external meson lines couple to baryon lines through the axial vector currents. This leaves only six topologically distinct one-loop diagrams, Fig.1, (out of thirteen in all) to calculate for the $s$-wave meson-nucleon scattering, apart from the usual radiative corrections in external lines. Since we are working to $\mathcal{O}(Q^3)$, only $\mathcal{L}^{(1)}$ enters into the loop calculation. Loops involving other terms can contribute at $\mathcal{O}(Q^4)$ or higher. The next term $\mathcal{L}^{(2)}$ contributes terms at order $\nu = 2$, that is, at tree order. These will be determined by the $KN$ sigma term and terms that could be calculated by resonance saturation. There are some uncertainties here as we shall point out later, but they turn out to be quite insignificant in the results. The next terms in $\mathcal{L}^{(3)}$ remove the divergences in the one-loop contributions and involve two finite counter terms – made up of two linear combinations of the many parameters appearing in the Lagrangian – that are to be determined empirically. As we will mention later, these constants are determined solely by isospin-odd amplitudes, the loop contribution to isospin-even amplitudes being free of divergences.

## 3 KN Scattering Amplitudes

### 3.1 On-shell amplitudes

The complete on-shell s-wave KN scattering amplitudes calculated to N$^2$LO ($\mathcal{O}(Q^3)$) [2] read

$$\begin{aligned} a_0^{K^\pm p} &= \frac{m_B}{4\pi f^2(m_B+M_K)}\left[\mp M_K + (\bar{d}_s+\bar{d}_v)M_K^2 + \{(L_s+L_v)\pm(\bar{g}_s+\bar{g}_v)\}M_K^3\right] \\ &\quad +\delta a_{\Lambda^\star}^{K^\pm p} \\ a_0^{K^\pm n} &= \frac{m_B}{4\pi f^2(m_B+M_K)}\left[\mp\frac{1}{2}M_K + (\bar{d}_s-\bar{d}_v)M_K^2 + \{(L_s-L_v)\pm(\bar{g}_s-\bar{g}_v)\}M_K^3\right] \end{aligned} \quad (6)$$

where $\bar{d}_s$ is the t-channel isoscalar contribution of $\mathcal{O}(Q^2)$, and $\bar{d}_v$ is the t-channel isovector one of $\mathcal{O}(Q^2)$:

$$\begin{aligned} \bar{d}_s &= -\frac{1}{2B_0}(a_1+2a_2+4a_3)+\frac{1}{4}(d_1+d_2+d_7+d_8)+\frac{1}{2}(d_3+d_4)+d_5+d_6 \\ \bar{d}_v &= -\frac{1}{2B_0}a_1+\frac{1}{4}(d_1+d_2+d_7+d_8) \end{aligned} \quad (7)$$

with $B_0 = M_K^2/(\hat{m}+m_s)$ where $M_K$ is the kaon mass and $\hat{m} = (m_u+m_d)/2$. Here $\delta a_{\Lambda^\star}^{K^\pm p}$ is the contribution from the $\Lambda^\star$ to be specified below and $L_s(L_v)$ is the finite crossing-even t-channel isoscalar (isovector) one-loop contribution

$$\begin{aligned} L_s M_K &= \frac{1}{128\pi f^2 M_K^2}\left(\frac{1}{3}(D-3F)^2(M_\pi^2+3M_\eta^2)M_\eta - 9M_K^2\sqrt{M_\eta^2-M_K^2}\right) \\ &\approx -0.109 \text{ fm} \\ L_v M_K &= \frac{1}{128\pi f^2 M_K^2}\left(-\frac{1}{3}(D+F)(D-3F)(M_\pi^2+3M_\eta^2)(M_\pi+M_\eta) - 3M_K^2\sqrt{M_\eta^2-M_K^2}\right. \\ &\qquad \left. -\frac{1}{6}(D+F)(D-3F)(M_\pi^2+3M_\eta^2)(M_\pi^2+M_\eta^2)\int_0^1 \frac{1}{\sqrt{(1-x)M_\pi^2+xM_\eta^2}}\right) \\ &\approx +0.021 \text{ fm} \end{aligned} \quad (8)$$

where $f = 93MeV$ and physical masses are used to obtain the numbers. The quantity $\bar{g}_s(\bar{g}_v)$ is the crossing-odd t-channel isoscalar (isovector) contribution from one-loop plus counter terms which after the dimensional regularization specified in Appendix C, takes the form

$$\bar{g}_{s,v} = \alpha_{s,v}^r + \beta_{s,v}^r + \frac{1}{32\pi^2}\frac{1}{f^2M_K^2}\left(\gamma_{s,v} + \sum_{i=\pi,K,\eta}\delta_{s,v}^i \ln\frac{M_i^2}{\mu^2}\right) \quad (9)$$

where $\mu$ is the arbitrary scale parameter that enters in the dimensional regularization and $\alpha$ and $\beta$ are contributions from the counter terms in $\mathcal{O}(Q^3)$,[#2] and $\gamma$ and $\delta$ are finite loop contributions. The explicit forms of $\alpha$, $\beta$, $\gamma$ and $\delta$ are given in Appendix C. It should be noted that while $\alpha$ and $\beta$ are $\mu$-dependent, $\bar{g}$ is scale-independent. ($\gamma$ and $\delta$ are scale-independent numbers.) Thus if one

[#2] On-shell, one can combine $\alpha$ and $\beta$ into one set of parameter to be determined from experiments. Off-shell, however, they are multiplied by a different power of the frequency $\omega$ as indicated in Appendix E and hence represent two independent parameters. This introduces one unfixed parameter in the off-shell case. However it turns out that the off-shell amplitudes are rather insensitive to the precise values of these constants, so we set (somewhat arbitrarily) $\alpha_{s,v}^r \approx \beta_{s,v}^r$ in our calculation, Figure 2.

fixes $\bar{g}$ from experiments, then for a given $\mu$, one can fix $\alpha+\beta$ at a fixed $\mu$. Equivalently, we can separate out the specific $\mu$-dependent terms so as to cancel the $\ln\mu$ term in eq.(9), thereby defining $\mu$-independent constants $\alpha'$ and $\beta'$

$$\alpha^r_{s,v}+\beta^r_{s,v}=\alpha'_{s,v}+\beta'_{s,v}-\frac{1}{32\pi^2}\frac{1}{f^2M_K^2}\sum_{i=\pi,K,\eta}\delta^i_{s,v}\ln\frac{M_i^2}{\mu^2} \tag{10}$$

and determine $\alpha'_{s,v}$ and $\beta'_{s,v}$ from experiments. From now on when we go off-shell (*i.e*, in Appendix E), we will drop the primes understanding that we are dealing with the $\mu$-independent parameters. (On-shell, this subtlety is not relevant since we can work directly with $\bar{g}$ of eq.(9).)

To understand the role of the $\Lambda^\star$, we observe that the measured scattering lengths are repulsive in all channels except $K^-n$ [22, 23]:[#3]

$$\begin{aligned} a_0^{K^+p}&=-0.31\text{ fm}, & a_0^{K^-p}&=-0.67+i0.63\text{ fm}\\ a_0^{K^+n}&=-0.20\text{ fm}, & a_0^{K^-n}&=+0.37+i0.57\text{ fm}. \end{aligned} \tag{11}$$

The repulsion in $K^-p$ scattering cannot be explained from eq.(6) without the $\Lambda^\star$ contribution. In fact it is well known that the contribution of the $\Lambda(1405)$ bound state gives the repulsion required to fit empirical data for s-wave $K^-p$ scattering [2, 24]. As mentioned, we may introduce the $\Lambda^\star$ as an elementary field. To the leading order in the chiral counting, it takes the form

$$\mathcal{L}_{\Lambda^\star} \;=\; \bar{\Lambda}^\star_v(iv\cdot\partial-m_{\Lambda^\star}+m_B)\Lambda^\star_v+\left(\sqrt{2}g_{\Lambda^\star}\,\mathrm{Tr}\,(\bar{\Lambda}^\star_v v\cdot AB_v)+\mathrm{h.\,c.}\right). \tag{12}$$

The coupling constant $g_{\Lambda^\star}$ can be fixed by the decay width $\Lambda^\star\to\Sigma\pi$ [2] if one ignores $SU(3)$ breaking

$$g^2_{\Lambda^\star}(pK^-)\approx g^2_{\Lambda^\star}(\Sigma\pi)\approx 0.15. \tag{13}$$

This is what one would expect at tree order. If one wants to go to one-loop order [25] corresponding to $\mathcal{O}(Q^3)$ at which $SU(3)$ breaking enters, then we encounter two counter terms $h^\star_{1,2}$,

$$\mathcal{L}^{\nu=3} \;=\; h^\star_1\sqrt{2}\bar{\Lambda}^\star_v\mathrm{Tr}\,(\chi_+ v\cdot AB_v)+h^\star_2\sqrt{2}\bar{\Lambda}^\star_v\mathrm{Tr}\,(\chi_+B_v v\cdot A)+h.c. \tag{14}$$

and the renormalized coupling to $\mathcal{O}(Q^3)$ will take the form

$$\begin{aligned} g^r_{\Lambda^\star}(\Sigma\pi) &= g_{\Lambda^\star}+\sum_{i=\pi,K,\eta}\alpha_i^{\Sigma\pi}\ln\frac{M_i^2}{\mu^2}+\beta^{\Sigma\pi}+2\,(h_1^{\star r}+h_2^{\star r})\hat{m}\\ g^r_{\Lambda^\star}(pK^-) &= g_{\Lambda^\star}+\sum_{i=\pi,K,\eta}\alpha_i^{pK^-}\ln\frac{M_i^2}{\mu^2}+\beta^{pK^-}+2\,(h_1^{\star r}m_s+h_2^{\star r}\hat{m}) \end{aligned} \tag{15}$$

where $\alpha_i$ and $\beta$ are calculable loop contributions. In [25], Savage notes that if one ignores the counter terms, then the finite log terms would imply that $g_{\Lambda^\star}(pK^-)$ would come out to be considerably smaller than $g_{\Lambda^\star}(\Sigma\pi)$, presumably due to an $SU(3)$ breaking. In our approach we choose to pick

[#3] Although the experimental $K^-N$ scattering lengths are given with error bars, the available $K^+N$ data are not very well determined. Since both are used in fitting the parameters of the Lagrangian, we do not quote the error bars here and shall not use them for fine-tuning. For our purpose, we do not need great precision in the data as the results are extremely robust against changes in the parameters.

the constants from experiments since we see no reason to suppose that the counter terms are zero and furthermore the presently available data[23] give

$$(g^2_{\Lambda^\star}(pK^-))_{exp} \approx 0.25 \tag{16}$$

which is *bigger* than the $SU(3)$ value (13). We will take this value in our calculation. It should also be mentioned that the Callan-Klebanov skyrmion predicts a value close to (13) [26]. The $\Lambda^\star$ contribution to the kaon-proton scattering amplitude is now completely determined,

$$\delta a^{K^\pm p}_{\Lambda^\star} = -\frac{m_B}{4\pi f^2(m_B+M_K)}\left[\frac{g^2_{\Lambda^\star}M_K^2}{m_B \mp M_K - m_{\Lambda^\star}}\right]. \tag{17}$$

To one-loop order, the $\Lambda^\star$ mass picks up an imaginary part through the graph $\Lambda^\star \to \Sigma\pi \to \Lambda^\star$. In our numerical work we will take $m_{\Lambda^\star}$ to be complex. The presence of the imaginary part explains that the empirical coupling constant (16) is bigger than the $SU(3)$ value (13).

We are left with four parameters in (6), $\bar{d}_s, \bar{d}_v, \bar{g}_s$ and $\bar{g}_v$, which we can determine with the four experimental (real parts of) scattering lengths (11). The results are

$$\begin{aligned} \bar{d}_s &\approx 0.201 \text{ fm}, \qquad & \bar{d}_v &\approx 0.013 \text{ fm}, \\ \bar{g}_s M_K &\approx 0.008 \text{ fm}, \qquad & \bar{g}_v M_K &\approx 0.002 \text{ fm}. \end{aligned} \tag{18}$$

The scattering amplitudes in each chiral order are given in Table 1. One sees that while the order $Q$ and order $Q^2$ terms are comparable, the contribution of order $Q^3$ is fairly suppressed relative to them. As a whole, the subleading chiral corrections are verified to be consistent with the "naturalness" condition as required of effective field theories. Using other sets of values of $f$, $D$ and $F$ does not change $L_s$ and $L_v$ significantly and leave unaffected our main conclusion. As expected, the $\Lambda^\star$ plays a predominant role in $K^-p$ scattering near threshold. This indicates that it will be essential in describing kaon-nuclear interactions, e.g., kaonic atoms.

### 3.2 Off-Shell Amplitudes

We now turn to off-shell s-wave $K^-$ forward scattering off static nucleons. The kinematics involved are $t = 0$, $q^2 = q'^2 = \omega^2$, $s = (m_B + \omega)^2$ with an arbitrary (off-shell) $\omega$. (See Appendix E.)

In going off-shell, we need to separate different kinematic dependences of the constant $\bar{d}_{s,v}$ of eq.(7) which consists of what would correspond to the KN sigma term $\Sigma_{KN}$ at tree order, $\sigma_{KN}(\approx \Sigma_{KN}) \equiv -\frac{1}{2}(\hat{m}+m_s)(a_1+2a_2+4a_3)$ involving the quark mass matrix $\mathcal{M}$, and the $d_i$ terms containing two time derivatives. The $\sigma_{KN}$ term, which gives an attraction, is a constant independent of the kaon frequency $\omega$, whereas the $d_i$ terms which are repulsive are proportional to $\omega^2$ in s-wave. In kaonic atoms and kaon condensation, the $\omega$ value runs down from its on-shell value $M_K$. This means that as $\omega$ goes down, the attraction stays unchanged and the repulsion gets suppressed. Thus while for on-shell amplitudes, they can be obtained independently of any assumptions, they need to be separated for off-shell amplitudes that we are interested in. If we could determine the KN sigma term from experiments, there would be no ambiguity. The trouble is that the sigma term extracted from experiments is not precise enough to be useful. The presently available value ranges

$$\Sigma_{KN} \sim (200-400) \text{ MeV}. \tag{19}$$

Here we choose to separate the two components by estimating the contributions to $d_i$ from the leading $1/m_B$ corrections with the octet and decuplet intermediate states in the relativistic Born graphs. As suggested by the authors of ref.[27] for $\pi N$ scattering, we might assume that the counter terms $d_i$ could equally be saturated by such intermediate states. This strategy is discussed in detail in Appendix D. This is somewhat like saturating the dimension-four counter terms $L_i$ in the chiral Lagrangian by resonances, a prescription which turns out to be surprisingly successful. The reason for believing that this might be justified in the present case is that the $\mathcal{O}(Q^2)$ terms are not affected by chiral loops, so must represent the degrees of freedom that are integrated out from the effective Lagrangian. But there are no known mechanisms that would contribute to $d_i$ other than the baryon resonances. When computed by resonance saturation, the contributions go like $1/m_B$. However this is not to be taken as $1/m_B$ corrections that arise as relativistic corrections to the static limit of a relativistic theory. The HFF as used in chiral perturbation theory does not correspond merely to a non-relativistic reduction although at low orders, they are equivalent. To be more specific, imagine starting with the following relativistic Lagrangian density

$$\mathcal{L}_{rel} \quad = \quad \cdots + e_i \mathrm{Tr}\,[\bar{B}\gamma_\mu A^\mu \gamma_\nu A^\nu B] + \cdots + f_i \mathrm{Tr}\,[D_\mu \bar{B} A^\mu A^\mu D_\mu B] + \cdots . \tag{20}$$

In going to the heavy-baryon limit, we get the $\mathcal{O}(Q^2)$ terms of the form

$$\mathcal{L}_v \quad = \quad \cdots + d_i \mathrm{Tr}\,[\bar{B}_v v\cdot A^2 B_v] + \cdots \tag{21}$$

with $d_i = (d_{\frac{1}{m}} + e_i + m_B^2 f_i + \cdots)$ where $d_{\frac{1}{m}}$ is the calculable $1/m_B$ correction from the relativistic leading-order Lagrangian. Clearly the $e_i$ and $f_i$ terms cannot be computed [25]. Thus if one imagines that the constants $d_i$ are infested with the terms of the latter form, there is no way that one can estimate these constants. While this introduces an element of uncertainty in our calculation, it does not seriously diminish the predictivity of the theory: Much of the uncertainty are eliminated in our determination of the parameters by experimental data. From eq.(18) and the $d_i$ terms estimated in Appendix D, we can extract the parameter[#4]

$$\sigma_{KN} \approx 2.83 M_\pi . \tag{22}$$

This *parameter* will be used for off-shell KN scattering amplitudes and kaon self-energy.

The predicted off-shell $K^-p$ and $K^-n$ scattering amplitudes are shown in solid line in Figure 2 for the range of $\sqrt{s}$ from 1.3 GeV to 1.5 GeV with $g^2_{\Lambda^\star} = 0.25$ and $\Gamma_{\Lambda^\star} = 50$ MeV taken from experiments. (The dotted lines in Fig.2 are explained in Appendix D.) The explicit formulas are listed in Appendix E. The $K^-n$ scattering is independent of the $\Lambda^\star$ and so the amplitude varies smoothly over the range involved.[2] Our predicted $K^-p$ amplitude is found to be in fairly good agreement with the empirical fit of ref.[21]. The striking feature of the real part of the $K^-p$ amplitude, repulsive above and attractive below $m_{\Lambda^\star}(1405MeV)$ as observed here, and the $\omega$-independent attraction of the $K^-n$ amplitude are relevant to kaonic atoms [18] and to kaon condensation in "nuclear star" matter. The imaginary part of the $K^-p$ amplitude is somewhat too high compared with the empirical fits. This may have to do with putting the experimental $\Lambda^\star$ decay width for the imaginary part of the mass. Self-consistency between loop corrections and the imaginary part of the mass would have to be implemented to get the correct imaginary part of the $K^-p$ amplitude.

[#4] This is not the *sigma term* $\Sigma_{KN} = \frac{1}{2}(\bar{m} + m_s)\langle P|\bar{u}u + \bar{s}s|P\rangle$. There are loop corrections to be added to this value.

### 3.3 Adler soft-meson conditions

The off-shell amplitude calculated here does not satisfy Adler's soft-meson conditions that follow from the usual PCAC assumption that the pseudoscalar meson field $\pi$ interpolate as the divergence of the axial current. The chiral Lagrangian used here does not give the direct relation $\pi^i \sim \partial_\mu J_5^{i\mu}$ where $J_5^{i\mu}$ is the axial current with flavor index $i$. Therefore in the soft-meson limit which corresponds in the present case to setting $\omega$ equal to zero, the $\pi N$ amplitude is not given by $-\frac{\Sigma_{\pi N}}{f^2}$ as it does in the case of Adler's interpolating field [28]. In fact, it gives $\frac{\Sigma_{\pi N}}{f^2}$ which has the opposite sign to Adler's limit. This led several authors to raise the possibility that a different physics might be involved in the chiral perturbation description of the off-shell processes that take place near $\omega = 0$ [10, 11].

A simple answer to this issue is that physics should not depend upon the interpolating field for the Goldstone bosons $\pi$ [29]. The physics is equivalent whether one uses the $\pi$ field as defined by the chiral Lagrangian used here or the $\pi' \propto \partial_\mu J_5^\mu$ field that gives Adler's conditions. Both are interpolating fields and they are just field-redefinitions of each other. This is natural since the Goldstone boson field is an auxiliary field in QCD. An explicit illustration of the equivalence in the case considered in this paper is given in Appendix F, to which skeptics are referred. Let it suffice here to say that if one wishes, one could rewrite the effective Lagrangian in such a way that Ward-Takahashi identities, to which Adler's conditions belong, are satisfied, without changing the physics involved. See ref. [30].

## 4 Kaon Self-Energy and Kaonic Atom

If one were to limit oneself to linear density approximation which would be reliable in dilute systems, then what we have obtained so far is sufficient for studying kaon-nucleon interactions in many-body systems. The off-shell KN amplitude calculated to $\mathcal{O}(Q^3)$ in impulse approximation gives the optical potential, which, expressed as a self-energy, is depicted by Fig.3a,

$$\Pi_K^{imp}(\omega) \;=\; -\Big(\rho_p \mathcal{T}_{free}^{K^- p}(\omega) + \rho_n \mathcal{T}_{free}^{K^- n}(\omega)\Big) \tag{23}$$

where $\mathcal{T}^{KN}$ is the off-shell s-wave KN transition matrix [#5]. For the purpose of studying kaon condensation, the linear density approximation may not be reliable enough and one would have to study the *effective action* (or *effective potential* in translationally invariant systems).

To go beyond the linear density approximation, there are two major effects to be considered. The first is the Pauli correction and the second is many-body correlations.

The Pauli effect can be most straightforwardly taken into account in the self-energy by modifying the nucleon propagator in the loop graphs contributing to the KN scattering amplitude to one appropriate in medium

$$G^0(k) \simeq \frac{i}{v\cdot k + i\epsilon} - 2\pi\delta(k_0)\theta(k_F - |\vec{k}|) \tag{24}$$

where $k_F$ is the nucleon Fermi momentum related to density $\rho_N$ by the usual relation $\rho_N = \frac{\gamma}{6\pi^2}k_{F_N}^3$ with the degeneracy factor $\gamma = 2$ for neutron and proton in nuclear matter. The resulting correction

[#5] The amplitude $\mathcal{T}^{KN}$ taken on-shell, *i.e.*, $\omega = M_K$, and the scattering length $a^{KN}$ are related by $a^{KN} = \frac{1}{4\pi(1+M_K/m_B)}\mathcal{T}^{KN}$.

denoted $\delta\mathcal{T}^{K^-N}_{\rho N}$ and given explicitly in Appendix G is clearly nonlinear in density and repulsive as befits a Pauli exclusion effect.

For the second effect, the most important one is the correlation involving "particle-hole" excitations. This is of typically many-body nature. There are two classes of correlations one would have to consider. One involves non-strange particle-hole excitations and the other strange particle-nonstrange hole excitations. All these can be mediated by four-Fermi interactions described above.

We first consider the latter. These are depicted in Fig. 4. Since we are dealing with s-wave kaon interaction, the most important configuration that $K^-$ can couple to is the $\Lambda^\star$ particle-nucleon hole (denoted as $\Lambda^\star N^{-1}$ with $N$ either a proton ($p$) or neutron ($n$)). We shall return to nonstrange particle-hole correlations when we treat density effects on the basic constants of the Lagrangian (*i.e*, "BR scaling"). Here we focus on the former type. Now for the s-wave in-medium kaon self-energy, the relevant four-Fermi interactions that involve a $\Lambda^\star$ can be reduced to a simple form involving two unknown constants

$$\mathcal{L}_{4-fermion} = C^S_{\Lambda^\star}\bar{\Lambda}^\star_v\Lambda^\star_v\mathrm{Tr}\ \bar{B}_vB_v + C^T_{\Lambda^\star}\bar{\Lambda}^\star_v\sigma^k\Lambda^\star_v\mathrm{Tr}\ \bar{B}_v\sigma^kB_v \tag{25}$$

where $C^{S,T}_{\Lambda^\star}$ are the dimension $-2$ ($M^{-2}$) parameters to be fixed empirically and $\sigma^k$ acts on baryon spinor.

Additional (in-medium) two-loop graphs that involve $\Lambda^\star N^{-1}$ excitations are given in Fig. 4c. They do not however involve contact four-Fermi interactions, so are calculable unambiguously.

We shall denote the sum of these contributions from Figs. 4 to the self-energy by $\Pi_{\Lambda^\star}$. A simple calculation gives

$$\begin{aligned}\Pi_{\Lambda^\star}(\omega) &= -\frac{g^2_{\Lambda^\star}}{f^2}\left(\frac{\omega}{\omega+m_B-m_{\Lambda^\star}}\right)^2\left\{C^S_{\Lambda^\star}\rho_p\left(\rho_n+\frac{1}{2}\rho_p\right)-\frac{3}{2}C^T_{\Lambda^\star}\rho^2_p\right\}\\ &\quad -\frac{g^4_{\Lambda^\star}}{f^4}\rho_p\left(\frac{\omega}{\omega+m_B-m_{\Lambda^\star}}\right)^2\omega^2\left(\Sigma^p_K(\omega)+\Sigma^n_K(\omega)\right)\end{aligned} \tag{26}$$

where $g_{\Lambda^\star}$ is the renormalized $KN\Lambda^\star$ coupling constant determined in [2] and $\Sigma^N_K(\omega)$ is given by

$$\Sigma^N_K(\omega) = \frac{1}{2\pi^2}\int_0^{k_{F_N}} d|\vec{k}|\frac{|\vec{k}|^2}{\omega^2-M^2_K-|\vec{k}|^2}. \tag{27}$$

In eq.(26), the first term comes from the diagrams of Figs. 4a and 4b and the second term from the diagram of Fig. 4c. While the second term gives repulsion corresponding to a Pauli quenching, the first term can give either attraction or repulsion depending on the sign of $(C^S_{\Lambda^\star}[\rho_n+\frac{1}{2}\rho_p]-\frac{3}{2}C^T_{\Lambda^\star}\rho_p)$ with the constants $C^{S,T}_{\Lambda^\star}$ being the only parameters that are not determined by on-shell data.

The complete self-energy to in-medium two-loop order is then

$$\Pi_K(\omega) = -\left(\rho_p\mathcal{T}^{K^-p}_{free}(\omega)+\rho_n\mathcal{T}^{K^-n}_{free}(\omega)\right)-\left(\rho_p\delta\mathcal{T}^{K^-p}_{\rho_N}(\omega)+\rho_n\delta\mathcal{T}^{K^-n}_{\rho_N}(\omega)\right)+\Pi_{\Lambda^\star}(\omega). \tag{28}$$

The additional parameters $C^{S,T}_{\Lambda^\star}$ that are introduced at the level of four-Fermi interactions in the strange particle-hole sector require experimental data involving nuclei and nuclear matter. We shall now discuss how these constants can be fixed from kaonic atom data. In order to fix both of these constants, we would need data over a wide range of nuclei. One sees in (26) that for the symmetric matter, what matters is the combination $(C^S_{\Lambda^\star}-C^T_{\Lambda^\star})$. At present, this is the only

combination that we can hope to pin down from kaonic atom data. That leaves one parameter unfixed. We shall pick $C^S_{\Lambda^\star}$ for the reason to be explained later. We shall parametrize the proton and neutron densities by the proton fraction $x$ and the nucleon density $u = \rho/\rho_0$ as

$$\rho_p = x\rho\ ,\quad \rho_n = (1-x)\rho\ ,\quad \rho = u\rho_0. \tag{29}$$

Now what we know from the presently available kaonic atom data [18] is that the optical potential for the $K^-$ in medium has an attraction of the order of

$$\Delta V \approx -(180 \pm 20)\ \ \text{MeV}\ \ at\ \ u = 0.97. \tag{30}$$

This implies approximately for $x = 1/2$

$$(C^S_{\Lambda^\star} - C^T_{\Lambda^\star})f^2 \approx 10. \tag{31}$$

Table 2 gives details of how this value is arrived at. It also lists the contributions of each chiral order to the self-energy (28), $\Delta V = M^\star_K - M_K$ and $M^\star_K$ which we shall loosely call "effective kaon mass" #6

$$M^\star_K \equiv \sqrt{M^2_K + \Pi_K}. \tag{32}$$

To exhibit the role of $\Lambda^\star$ in the kaon self-energy, we list each contribution of $\Pi$. Here $\Pi_{free} = -\rho_N \mathcal{T}^{K^-N}_{free}$, $\delta\Pi = -\rho_N \delta\mathcal{T}^{K^-N}$, $\Pi^1_{\Lambda^\star}$ corresponds to the first term of eq.(26) which depends on $C^{S,T}_{\Lambda^\star}$ and $\Pi^2_{\Lambda^\star}$ to the second term independent of $C^{S,T}_{\Lambda^\star}$. We observe that the $C^{S,T}_{\Lambda^\star}$-dependent term plays a crucial role for attraction in kaonic atom.

In Table 3 and Fig. 5, we list the predicted density dependence of the real part of the kaonic atom potential for $x = 0.5$ obtained for $(C^S_{\Lambda^\star} - C^T_{\Lambda^\star})f^2 \approx 10$.

To understand what the remaining parameter $C^S_{\Lambda^\star}$ is physically, we consider the mass shift of the $\Lambda^\star$ in medium. To one-loop order, there are two graphs given in Fig.6. A simple calculation gives

$$\delta m_{\Lambda^\star} = \sum_{i=a,b} \delta\Sigma^{(i)}_{\Lambda^\star}(\omega = m_{\Lambda^\star} - m_B) \tag{33}$$

where

$$\begin{aligned} \delta\Sigma^{(a)}_{\Lambda^\star}(\omega) &= -\frac{g^2_{\Lambda^\star}}{f^2}\omega^2\left(\Sigma^p_K(\omega) + \Sigma^n_K(\omega)\right) \\ \delta\Sigma^{(b)}_{\Lambda^\star}(\omega) &= -C^S_{\Lambda^\star}(\rho_p + \rho_n). \end{aligned} \tag{34}$$

The superscript $(a,b)$ stands for the figures (a) and (b) of Fig. 6. The contribution from Fig.6a is completely given with the known constants. The dependence on the unknown constant $C^S_{\Lambda^\star}$ appears linearly in the Fig.6b. For the given values adopted here, the mass shift is numerically

$$\delta m_{\Lambda^\star}(u,x,y) = [r(u,x) - 150.3 \times u \times y]\ \ \text{MeV} \tag{35}$$

where $y = C^S_{\Lambda^\star} f^2$ and $r(u,x) \equiv \delta\Sigma^{(a)}_{\Lambda^\star}$ with the numerical values given in Table 4.

#6 This is not, strictly speaking, a mass but we shall refer to it as such in labeling the figures.

One can see from eq.(35) and Table 4 that the shift in the $\Lambda^\star$ mass in medium is primarily controlled by the constant $C^S_{\Lambda^\star}$. For symmetric matter ($x = 1/2,\ u = 1$), the shift is zero for $y = 0.41$ and linearly dependent on the $y$ value for non-symmetric matter. At present we have no information as to whether the medium lowers or raises the mass of the $\Lambda^\star$, so it is really a free parameter but it is reasonable to expect that if any the shift cannot be very significant. We consider therefore that a reasonable value for $y$ is $\mathcal{O}(1)$.

In Table 5 and Fig.5 are given the properties of $K^+$ in nuclear matter. The self-energy of $K^+$ is simply obtained from that of $K^-$ by crossing $\omega \to -\omega$. One can note here that the interaction of $K^+$ with nuclear medium is quite weak as predicted by phenomenological models and supported by experiments. The $M^\star_K$ grows slowly as a function of density.[#7] This is a check of the consistency of the chiral expansion approach to kaon-nuclear interactions.

## 5 Critical Density for Kaon Condensation

We have now all the ingredients needed to calculate the critical density for negatively charged kaon condensation in dense nuclear star matter. For this, we will follow the procedure given in [9]. As argued in [6], we need not consider pions when electrons with high chemical potential can trigger condensation through the process $e^- \to K^-\nu_e$. Thus we can focus on the spatially uniform condensate

$$\langle K^-\rangle = v_K e^{-i\mu t} \tag{36}$$

where $\mu$ is the chemical potential which is equal, by Baym's theorem [33], to the electron chemical potential. The energy density $\tilde{\epsilon}$ – which is related to the effective potential in the standard way – is given by,

$$\begin{aligned}\tilde{\epsilon}(u,x,\mu,v_K) &= \frac{3}{5}E_F^{(0)}u^{\frac{5}{3}}\rho_0 + V(u) + u\rho_0(1-2x)^2S(u)\\ &\quad -[\mu^2 - M_K^2 - \Pi_K(\mu,u,x)]v_K^2 + \sum_{n\geq 2}a_n(\mu,u,x)v_K^n\\ &\quad +\mu u\rho_0 x + \tilde{\epsilon}_e + \theta(|\mu| - m_\mu)\tilde{\epsilon}_\mu\end{aligned} \tag{37}$$

where $E_F^{(0)} = \left(p_F^{(0)}\right)^2/2m_B$ and $p_F^{(0)} = (3\pi^2\rho_0/2)^{\frac{1}{3}}$ are, respectively, Fermi energy and momentum at nuclear density. The $V(u)$ is a potential for symmetric nuclear matter as described in [34] which is presumably subsumed in contact four-Fermi interactions (and one-pion-exchange – nonlocal – interaction) in the non-strange sector as mentioned above. It will affect the equation of state in the condensed phase but not the critical density, so we will drop it from now on. The nuclear symmetry energy $S(u)$ – also subsumed in four-Fermi interactions in the non-strange sector – does play a role as we know from [34]: Protons enter to neutralize the charge of condensing $K^-$'s making

[#7] Recent heavy-ion experiments at Brookhaven[31] find that $K^+$'s come out of quark-gluon plasma with a temperature of order of 20 MeV which is much lower than the freeze-out temperature of $\sim 140$ MeV. To understand this phenomenon, there has to be a mechanism at high temperature and density that reduces the $K^+$ mass considerably. Within the framework adopted here, this can happen only if the strong repulsion due to the $\omega$ exchange lodged in the first term of $\mathcal{L}^{(1)}$, eq.(1), is strongly suppressed so that the attraction coming from the sigma term becomes operative, thereby reducing the mass. As discussed in a recent paper by Brown and Rho [32], this can indeed happen if the vector meson decouples at high temperature and density. Here we are not concerned with this regime.

the resulting compact star "nuclear" rather than neutron star as one learns in standard astrophysics textbooks. We take the form advocated in [34]

$$S(u) \;=\; \left(2^{\frac{2}{3}}-1\right)\frac{3}{5}E_F^{(0)}\left(u^{\frac{2}{3}}-F(u)\right)+S_0F(u) \tag{38}$$

where $F(u)$ is the potential contributions to the symmetry energy and $S_0 \simeq 30MeV$ is the bulk symmetry energy parameter. We use three different forms of $F(u)$ as in [34]

$$F(u)=u\ ,\quad F(u)=\frac{2u^2}{1+u}\ ,\quad F(u)=\sqrt{u}. \tag{39}$$

It will turn out that the choice of $F(u)$ does not significantly affect the critical density. The contributions of the filled Fermi seas of electrons and muons are[#8] [9]

$$\begin{aligned}\tilde{\epsilon}_e &= -\frac{\mu^4}{12\pi^2}\\ \tilde{\epsilon}_\mu &= \epsilon_\mu-\mu\rho_\mu=\frac{m_\mu^4}{8\pi^2}\left((2t^2+1)t\sqrt{t^2+1}-\ln(t^2+\sqrt{t^2+1})\right)-\mu\frac{p_{F_\mu}^3}{3\pi^2}\end{aligned} \tag{40}$$

where $p_{F_\mu}=\sqrt{\mu^2-m_\mu^2}$ is the Fermi momentum and $t=p_{F_\mu}/m_\mu$.

The ground-state energy prior to kaon condensation is obtained by extremizing the energy density $\tilde{\epsilon}$ with respect to $x$, $\mu$ and $v_K$:

$$\left.\frac{\partial\epsilon}{\partial x}\right|_{v_K=0}=0\ ,\quad \left.\frac{\partial\epsilon}{\partial\mu}\right|_{v_K=0}=0\ ,\quad \left.\frac{\partial\epsilon}{\partial v_K^2}\right|_{v_K=0}=0 \tag{41}$$

from which we obtain three equations corresponding, respectively, to beta equilibrium, charge neutrality and dispersion relation:

$$\begin{aligned}\mu &= 4(1-2x)S(u)\\ 0 &= -xu\rho_0+\frac{\mu^3}{3\pi^2}+\theta(\mu-m_\mu)\frac{p_{F_\mu}^3}{3\pi^2}\\ 0 &= D^{-1}(\mu,u,x)=\mu^2-M_K^2-\Pi_K(\mu,u,x)\equiv\mu^2-{M_K^\star}^2(\mu,u,x).\end{aligned} \tag{42}$$

The proton fractions $x(u)$ and chemical potentials $\mu$ prior to kaon condensation are plotted in Fig. 7 and Figs. $8\sim10$ for various choices of the symmetry energy $F(u)$. We have solved these equations using for the kaon self-energy (a) the linear density approximation, eq.(23) and (b) the full two-loop result, eq.(28). Table 6.(a) shows the case (a) for different symmetry energies eq.(39). We see that the precise form of the symmetry energy does not matter quantitatively. The corresponding "effective kaon mass" $M_K^\star$ is plotted vs. $u$ in Figs. $8\sim10$ in solid line. Note that even in this linear density approximation kaon condensation *does* take place, *albeit* at a bit higher density than obtained before.

For the value that seems to be required by the kaonic atom data, (31), the critical density comes out to be about $u_c\approx3$, rather close to the original Kaplan-Nelson value.

[#8] We ignore hyperon Fermi seas in this calculation. We do not expect them to be important for s-wave kaon condensation.

In Table 6.(b) and Figs. $8 \sim 10$ are given the predictions for a wide range of values for $C^S_{\Lambda^\star} f^2$. What is remarkable here is that while the $C^{S,T}_{\Lambda^\star}$-dependent four-Fermi interactions are *essential* for triggering kaon condensation, the critical density is quite insensitive to their strengths. In fact, as one can see in Table 7, reducing the constant $(C^S_{\Lambda^\star} - C^T_{\Lambda^\star})f^2$ that represents the kaonic atom attraction by an order of magnitude to 1 with $C^S_{\Lambda^\star} f^2 = 10,\ 0$ modifies the critical density only to $u_c \approx 3.3,\ 4.5$, respectively.

To see how robust kaon condensation is with respect to the $\Lambda^\star KN$ coupling constant, let us take the extreme value $g^2_{\Lambda^\star} \approx 0.05$ used in [25] which gives the wrong sign to the $K^- p$ amplitude at threshold. In Table 8, $\Delta V$ of kaonic atom ($x = 0.5$) is given for $u = 0.97$ and for various choices of $(C^S_{\Lambda^\star} - C^T_{\Lambda^\star})f^2$. Constraining to the kaonic atom data implies approximately – within the range of error involved – $(C^S_{\Lambda^\star} - C^T_{\Lambda^\star})f^2 \approx 70$. In Table 9, the resulting critical densities are given for $(C^S_{\Lambda^\star} - C^T_{\Lambda^\star})f^2 \approx 70$, and those for other sets of $C^S_{\Lambda^\star}$ and $C^T_{\Lambda^\star}$ in Table 10. We see that given the constraint from kaonic atom data, the resulting critical densities are sensitive neither to the value of $C^{S,T}_{\Lambda^\star}$ nor to $g_{\Lambda^\star}$.

## 6 Four-Fermion Interactions and "Scaled" Chiral Lagrangians

So far we have ignored four-Fermi interactions in the non-strange sector with the understanding that the effects not involving strangeness are to be taken from what we know from nuclear phenomenology. From the chiral Lagrangian point of view, this is not satisfactory. One would like to be able to describe both the non-strange and strange sectors *on the same footing* starting from a three-flavor chiral Lagrangian. While recent developments indicate that nuclear forces may be understood at low energies in terms of a chiral Lagrangian [12, 13], it has not yet been possible to describe the ground-state property of nuclei including nuclear matter starting from a Lagrangian that has explicit chiral symmetry. So the natural question is: What about many-body correlations in the non-strange sector, not to mention those in the strange sector for which we are in total ignorance?

Montano, Politzer and Wise [20] addressed a related question in pion condensation in the chiral limit and found that four-Fermi interactions in the non-strange sector played an important role in inhibiting p-wave pion condensation in dense matter. It has of course been known since some time that the mechanism that quenches $g_A$ in nuclear matter to a value close to unity banishes the pion condensation density beyond the relevant regime. As shown in [35], this mechanism can be incorporated by means of a four-Fermi interaction in a chiral Lagrangian in a channel corresponding to the spin-isospin mode (that is, the Landau-Migdal $g'$ interaction).

In this section, we discuss a simple approach to including the main correlations in kaon condensation. We cannot do so in full generality to all orders in density but we can select what we consider to be the dominant ones by resorting to the scaling argument (which we shall call "BR scaling") introduced by Brown and Rho [32, 36].

How to implement the BR scaling in higher-order chiral expansion with the multiple scales that we are dealing with has not yet been worked out. It has up to date been formulated so as to be implemented *only at tree order* with the assumption that once the BR scaling is incorporated, higher-order terms are naturally suppressed. If this assumption is valid, which we can check à posteriori, by taking the BR scaling into account at tree order, that is, at $\mathcal{O}(Q^2)$ in our case, we

will be including most of higher-order density dependences through the simple scaling.

We first consider the leading-order ($\mathcal{O}(Q)$) term, which for s-wave kaon-nucleon interactions is given by the first term of eq.(1)

$$\sim \frac{1}{f^2} K^\dagger \partial_0 K B_v^\dagger B_v. \tag{43}$$

In terms of vector-meson exchanges, it is equivalent to an $\omega$-meson exchange, attractive in the $K^-$ channel and repulsive in the $K^+$ channel. Four-Fermi interactions in the non-strange channel can modify this interaction, the most important one being

$$\sim D\frac{1}{f^2} K^\dagger \partial_0 K (B_v^\dagger B_v)^2 \tag{44}$$

with $D$ an unknown constant. One may try to estimate the constant $D$ using dynamical models. For instance, one can have a four-Fermi interaction that arises when a massive scalar ($\sigma$ in the linear $\sigma$ model) is integrated out. This would increase the attraction of eq.(43) in the $K^-$ channel, which is equivalent to increasing the magnitude of $D$. One can also have a four-Fermi interaction that arises from integrating out a massive vector exchange of the $\omega$-meson quantum number, responsible for the screening of the attraction by a factor $(1+F_0)^{-1}$ where $F_0$ is the Landau-Migdal parameter $> 0$ in the density regime we are interested in [37]. This would decrease the magnitude of $D$. There are of course other terms but if we add them all up and write an effective two-Fermi interaction with correct symmetries by taking the mean-field $\langle \bar{B}_v B_v \rangle \approx \rho$, then the higher-density dependence is expected to modify (43) to

$$\sim \frac{1}{f^{\star 2}} K^\dagger \partial_0 K B_v^\dagger B_v \tag{45}$$

where the asterisk denotes density dependence $f^\star = f(\rho)$. Later we will assume this to be given by the BR scaling [32, 36]. Whether or not this assumption is viable will be tested *à posteriori*.

Similar four-Fermi interaction terms can also be written down for the $\mathcal{O}(Q^2)$ terms. However the effect here is expected to be less important for the following reason. First of all, the term involving the KN sigma term is associated with the strange quark property, in particular with the kaon decay constant $f_K$ and we expect that the $f_K$ is not modified significantly since the s-quark condensate does not change much as density and/or temperature is increased[38]. This implies that four-Fermi interactions will be less effective in modifying this term. The same must be the case with the counter terms $\bar{d}_i$ that are associated with the octet and decuplet of strange-quark flavor. We may assume them to be also unaffected by the renormalization.

In sum, *our proposition is that the net effect of multi-Fermi interactions in the non-strange sector can be summarized by the scaling $f \to f^\star$ in the leading term in (1).* As stated, we propose this scaling to be given by the BR scaling

$$\frac{f^\star}{f} \approx \frac{m_V^\star}{m_V} \approx 1 - cu \tag{46}$$

with $c \approx 0.15$. Since the multi-Fermi interactions are higher order in the chiral counting in terms of an expansion $k_F/\Lambda_\chi$, it is consistent to leave them out in the loop corrections, that is at $\mathcal{O}(Q^3)$.

The self-energy for kaonic atoms with the BR scaling is given in dashed line in Fig. 5 and tabulated in Tables 11 and 12. Comparing with Tables 2 and 3, we see that the BR scaling

gives only a slightly more attractive potential at low densities. The attraction, however, increases significantly at higher densities. From Table 11, we find for kaonic atoms, approximately,

$$(C^S_{\Lambda^\star} - C^T_{\Lambda^\star})f^2 \approx 10. \tag{47}$$

This is roughly the same as without the BR scaling since the scaling effect is not important at $u = 0.97$. The BR scaling becomes important in the region where condensation sets in. The corresponding critical density is given in Tables 13 and 14. The characteristic feature of the effect of the BR scaling is summarized in Figs.11, 12 and 13. The remarkable thing to notice is that the critical density lowered to $u_c \sim 2$ is completely insensitive to the parameters such as the form of the symmetry energy, the constants $C^{S,T}_{\Lambda^\star}$ etc. in which possible uncertainties of the theory lie.

In order to verify the key hypothesis of the BR scaling – that the scaling subsumes higher order effects, thus *suppressing* higher chiral order effects of the scaled Lagrangian, we keep all the parameters *fixed* at the values determined at $\mathcal{O}(Q^3)$, BR-scale as described above, then ignore all terms of $\mathcal{O}(Q^3)$ (*i.e*, loop corrections) and (A) set $C^S_{\Lambda^\star} = C^T_{\Lambda^\star} = 0$ and (B) set $(C^S_{\Lambda^\star} - C^T_{\Lambda^\star})f^2 = 10$ and calculate the critical density. The results are given in Table 15. We see that the effects of loop corrections and four-Fermi interactions amount to less than 10%. This may be taken as an *à posteriori* verification of the validity of the assumption made in deriving the scaling, although it is difficult to assess how reliable the absolute value of the predicted critical density (and the corresponding equation of state of the condensed phase) is.

# 7 Discussion

In conclusion, we have shown that chiral perturbation theory at order N$^2$LO predicts kaon condensation in "nuclear star" matter at a density $2 \lesssim u_c \lesssim 4$ with a large fraction of protons – $x = 0.1 \sim 0.2$ at the critical point and rapidly increasing afterwards – neutralizing the negative charge of the condensed kaons. For this to occur, four-Fermi interactions involving $\Lambda^\star$ are found to play an important role in driving the condensation but the critical density is negligibly dependent on the strength of the four-Fermi interaction.

It is found that the BR scaling [32, 36] favors a condensation at a density as low as twice the matter density and that when the BR scaling is operative, higher chiral corrections coming from the scaled Lagrangian are insignificant, justifying the basic assumption that goes into the derivation of the scaling relation. This suggest that at least for kaon condensation, the tree approximation with the scaled Lagrangian is consistent with the basic idea of the BR scaling.

Given the relatively low critical density obtained in the higher-order calculation of this paper, we consider it reasonable to assume that the compact-star properties will be qualitatively the same as in the tree-order calculation of ref. [9]. We will report on this matter in a future publication.

Our treatment is still far from self-consistent as there are many nuclear correlation effects that are still to be taken into account. How to incorporate them in full consistency with chiral symmetry is not known. In particular the role of four-Fermi interactions in the non-strange channel, *e.g.*., short-range nuclear correlations which involve both interaction terms in the Lagrangian and nuclear many-body effects, is still poorly understood. A problem of this sort may have to be addressed in terms of renormalization group flows as in condensed matter physics [39]. A work is in progress along this line [40].

## Acknowledgments

We acknowledge useful discussions with H. Jung, K. Kubodera, A. Manohar, F. Myhrer, V. Thorsson, A. Wirzba, W. Weise and H. Yabu. The work of CHL and DPM were supported in part by the Korea Science and Engineering Foundation through the CTP of SNU and in part by the Korea Ministry of Education under Grant No. BSRI-94-2418 and the work of GEB by the US Department of Energy under Grant No. DE-FG02-88ER40388.

## Appendix A: Vertices and Feynman Rules

In this Appendix, the chiral Lagrangian used is given explicitly in terms of the component fields (meson octet, baryon octet and decuplet) we are interested in. The vertices of the Feynman graphs can be read off directly. The subscript $n$ in $\mathcal{L}_n$ denotes the number of lines attached to the given vertex. In Fig.1, the three-point vertex $\mathcal{L}_3$ enters in the diagrams (c,d,f), the four-point vertices $\mathcal{L}_4^A$ (4-meson) and $\mathcal{L}_4^B$(2-meson + 2-baryon) in the diagrams (b,d) and (b,c,e), respectively and the higher-point vertices $\mathcal{L}_5$ and $\mathcal{L}_6$ figure in the diagrams (f) and (a), respectively.

$$
\begin{aligned}
\mathcal{L}_3 &= -\frac{1}{f}\Big[\bar{p}_v S_v^\mu p_v\left((D+F)\partial_\mu\pi^0-\frac{1}{\sqrt{3}}(D-3F)\partial_\mu\eta\right)\\
&\qquad +\bar{n}_v S_v^\mu n_v\left(-(D+F)\partial_\mu\pi^0-\frac{1}{\sqrt{3}}(D-3F)\partial_\mu\eta\right)\Big]\\
&\quad -\frac{1}{f}\Big[\sqrt{2}(D+F)\bar{p}_v S_v^\mu n_v\partial_\mu\pi^+ +\sqrt{2}(D-F)\bar{p}_v S_v^\mu\Sigma_v^+\partial_\mu K^0+\sqrt{2}(D-F)\bar{n}_v S_v^\mu\Sigma_v^-\partial_\mu K^+\\
&\qquad -\frac{1}{\sqrt{3}}(D+3F)\bar{p}_v S_v^\mu\Lambda_v\partial_\mu K^+-\frac{1}{\sqrt{3}}(D+3F)\bar{n}_v S_v^\mu\Lambda_v\partial_\mu K^0\\
&\qquad +(D-F)\bar{p}_v S_v^\mu\Sigma_v^0\partial_\mu K^+-(D-F)\bar{n}_v S_v^\mu\Sigma_v^0\partial_\mu K^0+h.c.\Big]\\
&\quad -\frac{C}{\sqrt{6}f}\Big[\sqrt{2}\bar{p}_v\partial^\mu\pi^0\Delta^+_{v,\mu}+\bar{p}_v\partial^\mu\pi^+\Delta^0_{v,\mu}+\frac{1}{\sqrt{2}}\bar{p}_v\partial^\mu K^+\Sigma^{*0}_{v,\mu}-\sqrt{3}\bar{p}_v\partial^\mu\pi^-\Delta^{++}_{v,\mu}\\
&\qquad -\bar{p}_v\partial^\mu K^0\Sigma^{*+}_{v,\mu}+\sqrt{2}\bar{n}_v\partial^\mu\pi^0\Delta^0_{v,\mu}-\bar{n}_v\partial^\mu\pi^-\Delta^+_{v,\mu}-\frac{1}{\sqrt{2}}\bar{n}_v\partial^\mu K^0\Sigma^{*0}_{v,\mu}\\
&\qquad +\sqrt{3}\bar{n}_v\partial^\mu\pi^+\Delta^-_{v,\mu}+\bar{n}_v\partial^\mu K^+\Sigma^{*-}_{v,\mu}+h.c.\Big]
\end{aligned}
\tag{A.1}
$$

$$
\begin{aligned}
\mathcal{L}_4^A &= -\frac{1}{6f^2}\Big[\frac{1}{2}\left((\pi^0+\sqrt{3}\eta)\overleftrightarrow{\partial}_\mu K^+\right)\left((\pi^0+\sqrt{3}\eta)\overleftrightarrow{\partial^\mu} K^-\right)\\
&\qquad +\left(-(K^+\overleftrightarrow{\partial}_\mu K^-)(\pi^+\overleftrightarrow{\partial^\mu}\pi^-)+(K^+\overleftrightarrow{\partial}_\mu\pi^-)(K^-\overleftrightarrow{\partial^\mu}\pi^+)\right)\\
&\qquad -(K^+\overleftrightarrow{\partial}_\mu K^-)(K^+\overleftrightarrow{\partial^\mu}K^-)\\
&\qquad +\left((K^+\overleftrightarrow{\partial}_\mu K^-)(\bar{K}^0\overleftrightarrow{\partial^\mu}K^0)+(K^+\overleftrightarrow{\partial}_\mu\bar{K}^0)(K^-\overleftrightarrow{\partial^\mu}K^0)\right)\Big]\\
&\quad +\frac{B_0}{6f^2}\Big[K^+K^-\left(\frac{1}{2}(3m_u+m_s)(\pi^0)^2+\frac{1}{\sqrt{3}}(m_u-m_s)\pi^0\eta+\frac{1}{2}(m_u+3m_s)\eta^2\right)\\
&\qquad +(2m_u+m_d+m_s)\pi^+\pi^-K^+K^-+(m_u+m_s)K^+K^-K^+K^-\\
&\qquad +(m_u+m_d+2m_s)K^+K^-\bar{K}^0K^0\Big]
\end{aligned}
\tag{A.2}
$$

$$
\begin{aligned}
\mathcal{L}_4^B &= -\frac{i}{4f^2}\Big[(K^+\overleftrightarrow{\partial}_\mu K^-)\left(2\bar{\Xi}_v^-v^\mu\Xi_v^- -\bar{\Sigma}_v^+v^\mu\Sigma_v^+ +\bar{\Sigma}_v^-v^\mu\Sigma_v^- +\bar{\Xi}_v^0v^\mu\Xi_v^0-2\bar{p}_vv^\mu p_v-\bar{n}_vv^\mu n_v\right)\\
&\qquad -\bar{p}_vv^\mu p_v\left\{\left(\pi^+\overleftrightarrow{\partial}_\mu\pi^-\right)-\left(\bar{K}^0\overleftrightarrow{\partial}_\mu K^0\right)\right\}+\bar{n}_vv^\mu n_v\left\{\left(\pi^+\overleftrightarrow{\partial}_\mu\pi^-\right)-2\left(K^0\overleftrightarrow{\partial}_\mu\bar{K}^0\right)\right\}\Big]\\
&\quad +\frac{i}{4f^2}\Big[\bar{p}_vv^\mu n_v\left(K^+\overleftrightarrow{\partial}_\mu\bar{K}^0\right)-\bar{\Sigma}_v^+v^\mu p_v\left(K^-\overleftrightarrow{\partial}_\mu\pi^+\right)-\frac{1}{\sqrt{2}}\bar{n}_vv^\mu\Sigma_v^-\left((\pi^0+\sqrt{3}\eta)\overleftrightarrow{\partial}_\mu K^+\right)
\end{aligned}
$$

$$
\begin{aligned}
&+\frac{1}{\sqrt{2}}\bar{n}_v v^\mu \left(\Sigma_v^0 - \sqrt{3}\Lambda_v\right)\left(\pi^- \overleftrightarrow{\partial}_\mu K^+\right) - \frac{1}{2}\bar{p}_v v^\mu \left(\Sigma_v^0 + \sqrt{3}\Lambda_v\right)\left((\pi^0 + \sqrt{3}\eta) \overleftrightarrow{\partial}_\mu K^+\right) \\
&+ h.c.\Big] \\
&-i\frac{3}{4f^2}\left[\left(K^+ v\cdot \overleftrightarrow{\partial} K^-\right)\left(\bar{\Delta}^{++}_{v,\nu}\Delta^{++,\nu}_v + \frac{2}{\sqrt{3}}\bar{\Delta}^{+}_{v,\nu}\Delta^{+,\nu}_v + \frac{1}{\sqrt{3}}\bar{\Sigma}^{*+}_{v,\nu}\Sigma^{*+,\nu}_v + \frac{1}{\sqrt{3}}\bar{\Delta}^{0}_{v,\nu}\Delta^{0,\nu}_v\right.\right. \\
&\left.\left. -\frac{1}{\sqrt{3}}\bar{\Xi}^{*0}_{v,\nu}\Xi^{*0,\nu}_v - \frac{1}{\sqrt{3}}\bar{\Sigma}^{*-}_{v,\nu}\Sigma^{*-,\nu}_v - \bar{\Omega}^{-}_{v,\nu}\Omega^{-,\nu}_v - \frac{2}{\sqrt{3}}\Xi^{*-}_{v,\nu}\Xi^{*-,\nu}_v\right)\right] \qquad \text{(A.3)}
\end{aligned}
$$

$$
\begin{aligned}
\mathcal{L}_5 \;=\; & \frac{1}{6\sqrt{2}f^3}\Bigg[ K^+K^-\left\{\sqrt{2}\bar{p}_v S_v^\mu p_v 2F(\partial_\mu\pi^0 + \sqrt{3}\partial_\mu\eta) - \sqrt{2}\bar{n}_v S_v^\mu n_v (D-F)(\partial_\mu\pi^0 + \sqrt{3}\partial_\mu\eta)\right\} \\
&+K^+K^-\Big\{ (D+F)\bar{p}_v S_v^\mu n_v \partial_\mu\pi^+ + (D-F)\bar{p}_v S_v^\mu \Sigma_v^+ \partial_\mu K^0 \\
&+2(D-F)\bar{n}_v S_v^\mu \Sigma_v^- \partial_\mu K^+ - \frac{2}{\sqrt{6}}(D+3F)\bar{p}_v S_v^\mu \Lambda_v \partial_\mu K^+ \\
&-\frac{1}{\sqrt{6}}(D+3F)\bar{n}_v S_v^\mu \Lambda_v \partial_\mu K^0 + \frac{2}{\sqrt{2}}(D-F)\bar{p}_v S_v^\mu \Sigma_v^0 \partial_\mu K^+ \\
&-\frac{1}{\sqrt{2}}(D-F)\bar{n}_v S_v^\mu \Sigma_v^0 \partial_\mu K^0 + h.c.\Big\}\Bigg] \\
&+\frac{C}{12\sqrt{2}f^3}\Bigg[ (K^+K^-)\left(\sqrt{\frac{2}{3}}\bar{p}_v\partial^\mu\pi^0\Delta^+_{v,\mu} + \sqrt{2}\bar{p}_v\partial^\mu\eta\Delta^+_{v,\mu} + \frac{1}{\sqrt{3}}\bar{p}_v\partial^\mu\pi^+\Delta^0_{v,\mu}\right. \\
&+\sqrt{\frac{2}{3}}\bar{p}_v\partial^\mu K^+\Sigma^{*0}_{v,\mu} - \bar{p}_v\partial^\mu\pi^-\Delta^{++}_{v,\mu} - \frac{1}{\sqrt{3}}\bar{p}_v\partial^\mu K^0\Sigma^{*+}_{v,\mu} + \sqrt{\frac{2}{3}}\bar{n}_v\partial^\mu\pi^0\Delta^0_{v,\mu} \\
&+\sqrt{2}\bar{n}_v\partial^\mu\eta\Delta^0_{v,\mu} + \bar{n}_v\partial^\mu\pi^+\Delta^-_{v,\mu} + \frac{2}{\sqrt{3}}\bar{n}_v\partial^\mu K^+\Sigma^{*-}_{v,\mu} \\
&\left.-\frac{1}{\sqrt{3}}\bar{n}_v\partial^\mu\pi^-\Delta^+_{v,\mu} - \frac{1}{\sqrt{6}}\bar{n}_v\partial^\mu K^0\Sigma^{*0}_{v,\mu}\right) + h.c.\Bigg] \qquad \text{(A.4)}
\end{aligned}
$$

$$
\begin{aligned}
\mathcal{L}_6 \;=\; & -\frac{i}{96f^4}\Bigg[ \bar{p}_v v^\mu p_v \Big\{ (K^+ \overleftrightarrow{\partial}_\mu K^-)(5\pi^+\pi^- + 5\bar{K}^0K^0 + 8K^+K^- + (\pi^0)^2 + 2\sqrt{3}\pi^0\eta + 3\eta^2) \\
&+7K^+K^-(\pi^+ \overleftrightarrow{\partial}_\mu \pi^-) - 7(\bar{K}^0 \overleftrightarrow{\partial}_\mu K^0)K^+K^-\Big\} \\
&+\bar{n}_v v^\mu n_v \Big\{ (K^+ \overleftrightarrow{\partial}_\mu K^-)\left(\frac{(\pi^0)^2}{2} + \sqrt{3}\pi^0\eta + \frac{3}{2}\eta^2 - 2\pi^+\pi^- + 4K^+K^- + 7\bar{K}^0K^0\right) \\
&-5(\bar{K}^0 \overleftrightarrow{\partial}_\mu K^0)K^+K^- + 2K^+K^-(\pi^+ \overleftrightarrow{\partial}_\mu \pi^-)\Big\}\Bigg] \qquad \text{(A.5)}
\end{aligned}
$$

where the quark masses are related to the meson masses as

$$
M_\pi^2 = B_0(m_u + m_d) = 2B_0\hat{m}, \quad M_\eta^2 = \frac{2}{3}B_0(\hat{m} + 2m_s), \quad M_K^2 = B_0(\hat{m} + m_s). \qquad \text{(A.6)}
$$

The propagator for the baryon octet in HFF is $i/(v\cdot k)$, where $k^\mu$ is the residual momentum of the baryon as defined by $p^\mu = m_B v^\mu + k^\mu$ [17]. The propagator for the decuplet is also simplified to the form $[i/(v\cdot k - \delta_T)] \times (v^\mu v^\nu - g^{\mu\nu} - 4\frac{d-3}{d-1}S_v^\mu S_v^\nu)$. In the HFF, the spin operator takes the form $S_v^\mu S_v^\nu = \frac{1}{4}(v^\mu v^\nu - g^{\mu\nu}) + \frac{i}{2}\epsilon^{\mu\nu\alpha\beta}v_\alpha S_{v,\beta}$.

Given the vertices and the propagators, one can immediately write down the the integral entering in the diagram (e) of Fig.1,

$$\begin{aligned} I_i^E &= \frac{1}{i}\int \frac{d^nk}{(2\pi)^n}\frac{v\cdot(2q-k)}{v\cdot k+i\epsilon}\frac{v\cdot(q+q'-k)}{(q-k)^2-M_i^2+i\epsilon} \\ &= -(v\cdot q'+2v\cdot q)\Delta_i + 2v\cdot q v\cdot(q+q')\Sigma_i(v\cdot q) \end{aligned} \tag{A.7}$$

where

$$\begin{aligned} \Delta_i &= \frac{1}{i}\int \frac{d^nk}{(2\pi)^n}\mu^\epsilon\frac{1}{k^2-M_i^2+i\epsilon} = -\frac{M_i^2}{16\pi^2}\ln\frac{M_i^2}{\mu^2} - M_i^2 2L \\ \Sigma_i(\omega) &= \frac{1}{i}\int \frac{d^nk}{(2\pi)^n}\frac{1}{k^2-M_i^2+i\epsilon}\frac{1}{v\cdot k+\omega+i\epsilon} \\ &= \frac{1}{8\pi^2}\left[\omega\left(1-\ln\frac{M_i^2}{\mu^2}\right)+\bar{f}_i(\omega)\right] - 4\omega L. \end{aligned} \tag{A.8}$$

Here the divergent term $L$ and the finite loop term $\bar{f}_i(\omega)$ are given by

$$\begin{aligned} L &= \frac{1}{16\pi^2}\mu^{-\epsilon}\left(-\frac{2}{\epsilon}+\gamma-1-\ln 4\pi\right) \\ \bar{f}_i(\omega) &= \sqrt{\omega^2-M_i^2}\left(\ln\left|\frac{\omega-\sqrt{\omega^2-M_i^2}}{\omega+\sqrt{\omega^2-M_i^2}}\right| + i2\pi\theta(\omega-M_i)\right) \quad \text{for } |\omega|>M_i \\ &= -\sqrt{M_i^2-\omega^2}\left(\pi+2\tan^{-1}\frac{\omega}{\sqrt{M_i^2-\omega^2}}\right) \qquad \text{for } |\omega|<M_i. \end{aligned} \tag{A.9}$$

Note that $\bar{f}_i(\omega)$ has a kink at $\omega = M_i$, which explains the nontrivial behavior of the $KN$ scattering amplitude seen in Fig.2. In order to get one-loop results, we also need the following well-known integrals

$$\begin{aligned} J_i(q^2) &= \frac{1}{i}\int \frac{d^nk}{(2\pi)^n}\mu^\epsilon\frac{1}{k^2-M_i^2+i\epsilon}\frac{1}{(k-q)^2-M_i^2+i\epsilon} \\ &= -\frac{1}{16\pi^2}\left(1+\ln\frac{M_i^2}{\mu^2}\right) - 2L + \bar{J}_i(q^2) \end{aligned} \tag{A.10}$$

where

$$\bar{J}_i(t) = \frac{1}{16\pi^2}\left[2-\sqrt{1-4M_i^2/t}\ \ln\frac{\sqrt{1-4M_i^2/t}+1}{\sqrt{1-4M_i^2/t}-1}\right]. \tag{A.11}$$

All the integrals needed for the diagrams in Fig.1 can be obtained from $\Delta_i$, $J_i(q^2)$ and $\Sigma_i(\omega)$.

## Appendix B: Mass and Wave Function Renormalizations

At one-loop order, we need one counter term, $\mathcal{L}_c = -\delta m_B \mathrm{Tr}\,\bar{B}B$, to renormalize the nucleon mass. It does not affect $KN$ scattering amplitude, but it is needed to absorb the divergences

coming from one-loop self-energy graphs. The nucleon self-energy including the counter terms is

$$\begin{aligned}\Sigma_N(\omega) &= \delta m_B - 2a_1\hat{m} - 2a_2 m_s - 2a_3(m_s+2\hat{m}) - 2\omega\bar{h} - c_1\omega^3 \\ &\quad + \sum_i \frac{\lambda_i}{f^2}\mathcal{H}_i(\omega) + \sum_i \frac{4}{3}\frac{\lambda_{D,i}}{f^2}\mathcal{H}_i(\omega-\delta_T) \end{aligned} \tag{B.1}$$

where $\omega = v\cdot p - m_B v$ and

$$\begin{aligned}\bar{h} &= h_1\hat{m} + h_2 m_s + h_3(2\hat{m}+m_s) \\ \mathcal{H}_i(\omega) &= -\frac{1}{4}\left[\omega\Delta_i + (M_i^2-\omega^2)\Sigma_i(\omega)\right] \\ \Delta_i &= -\frac{M_i^2}{16\pi^2}\ln\frac{M_i^2}{\mu_{\rm d.r.}^2} - M_i^2 2L \\ \Sigma_i(\omega) &= \frac{1}{8\pi^2}\left[\omega\left(1-\ln\frac{M_i^2}{\mu_{\rm d.r.}^2}\right) - f_i(\omega)\right] - 4\omega L \\ f_i(\omega) &= \sqrt{M_i^2-\omega^2}\left(\pi + 2\sin^{-1}\frac{\omega}{M_i}\right) \\ L &= \frac{1}{16\pi^2}\mu_{\rm d.r.}^{-\epsilon}\left(-\frac{2}{\epsilon}+\gamma-1-\ln 4\pi\right)\end{aligned} \tag{B.2}$$

and the coefficients $\lambda_i$'s are

$$\begin{aligned}\lambda_\pi &= 3(D+F)^2 \\ \lambda_K &= \frac{1}{3}\left((D+3F)^2 + 9(D-F)^2\right) \\ \lambda_\eta &= \frac{1}{3}(D-3F)^2 \\ \lambda_{D,\pi} &= 4\lambda_{D,K} = 2C^2.\end{aligned} \tag{B.3}$$

Here $\mu_{\rm d.r.}$ stands for the arbitrary mass scale $\mu$ that arises in the dimensional regularization. One can compute $Z_0$ and $Z_3$ from $\Sigma_N(\omega)$ or write down the corresponding counter terms as in renormalizable theory, $(Z_0-1)m_B\mathrm{Tr}\,\bar{B}B$ and $(Z_3-1)\mathrm{Tr}\,\bar{B}iv\cdot\partial B$.[#9] However in a non-renormalizable theory such as ours, many counter terms enter at order by order, so it is more convenient to use the constraints on $\Sigma_N(\omega)$ directly. Using a physical scheme, the convenient constraints are

$$\Sigma_N(\omega)|_{\omega=0} = 0, \qquad \left.\frac{\partial\Sigma_N(\omega)}{\partial\omega}\right|_{\omega=0} = 0. \tag{B.4}$$

In this case, the $m_B$, that figures in the leading-order Lagrangian, can be identified as the physical baryon mass. The constant $\delta m_B$ is determined by the first constraint to absorb the divergence and $\bar{h}$, relevant for $KN$ scattering, can be fixed by the second constraint. The latter is explicitly given by

$$\begin{aligned}\left.\frac{\partial\Sigma_N(\omega)}{\partial\omega}\right|_{\omega=0} &= -2\bar{h} + \sum_i \frac{\lambda_i}{f^2}\left(-\frac{1}{4}\Delta_i + M_i^2\left.\frac{\partial\Sigma_i(\omega)}{\partial\omega}\right|_{\omega=0}\right) \\ &\quad + \sum_i \frac{4}{3}\frac{\lambda_{D,i}}{f^2}\left(-\frac{1}{4}\Delta_i + 2\delta_T\Sigma(-\delta_T) + (M_i^2-\delta_T^2)\left.\frac{\partial\Sigma_i(\omega)}{\partial\omega}\right|_{\omega=-\delta_T}\right).\end{aligned} \tag{B.5}$$

[#9] In standard notation, $Z_0$ ($Z_3$) corresponds to the mass (wave function) renormalization. The counter term $(Z_0-1)m_B\mathrm{Tr}\,\bar{B}B$ corresponds to $\delta m_B\mathrm{Tr}\,\bar{B}B$, and $(Z_3-1)\mathrm{Tr}\,\bar{B}iv\cdot\partial B$ to the $h_i$ terms in the $\nu=3$ Lagrangian.

The constraints

$$Z_N - 1 = \left.\frac{\partial \Sigma_N(\omega)}{\partial \omega}\right|_{\omega=0} = 0 \tag{B.6}$$

completely determine $\bar{h}$ as a function of $\mu_{\rm d.r.}$. One convenient choice is $\bar{h} = \bar{h}^r(\mu_{\rm d.r.}) + \sum_i \alpha_i L$ where $L$ is the divergent piece, and $\bar{h}^r$ is the finite part that includes the chiral log terms $\ln(M_i^2/\mu_{\rm d.r.}^2)$. The renormalized parameter $\bar{h}^r(\mu_{\rm d.r.})$ is related with each other at different scales $\mu_{\rm d.r.}$ through the relation

$$\frac{\bar{h}^r(\mu_{\rm d.r.} = \mu_1)}{\bar{h}^r(\mu_{\rm d.r.} = \mu_2)} = \sum \beta_i(\delta_T) \ln \frac{\mu_1}{\mu_2} \ . \tag{B.7}$$

Consider now kaon self-energy which we can write as

$$\Pi_K(q^2) \ = \ \sum_i \frac{\alpha_i}{12 f^2} \Delta_i + c.t. \tag{B.8}$$

where $\alpha_i$ are given by

$$\alpha_\pi = -3M_\pi^2, \quad \alpha_K = -6M_K^2, \quad \alpha_\eta = M_\pi^2. \tag{B.9}$$

In the physical scheme, the constraints are

$$\Pi_K(q^2)\Big|_{q^2=M_K^2} = 0, \quad Z_K - 1 = \left.\frac{\partial \Pi_K(q^2)}{\partial q^2}\right|_{q^2=M_K^2} = 0 \tag{B.10}$$

where $M_K$ is the physical kaon mass.[#10] Note however that the counter terms in kaon self-energy do not affect the $KN$ scattering directly. So we shall not need the explicit magnitudes of these counter terms for our purpose.

Finally the scattering amplitudes can be obtained simply by calculating the six topologically distinct diagrams of Fig. 1 using physical masses

$$\mathcal{T}^{KN} = \sum_{i=a,\ldots,f} \mathcal{T}_i^{KN}. \tag{B.11}$$

This is because there is no contribution from the mass and wave function renormalizations,

$$\mathcal{T}_{w.r}^{KN} = \alpha \frac{(1 - Z_N + 1 - Z_K)}{2f^2} v \cdot (q + q') \tag{B.12}$$

where $\alpha = 2$ for $K^+p$ and $\alpha = 1$ for $K^+n$.

## Appendix C: Renormalization of $\mathcal{O}(Q^3)$ Counter Terms

The quantity $\bar{g}_s(\bar{g}_v)$ is the crossing-odd t-channel isoscalar (isovector) contribution from one-loop plus counter terms which after the standard dimensional regularization, takes the form

$$\bar{g}_{s,v} = \alpha_{s,v} + \beta_{s,v} + \frac{1}{32\pi^2}\frac{1}{f^2 M_K^2}\gamma_{s,v} + \sum_{i=\pi,K,\eta} \delta_{s,v}^i \frac{1}{f^2 M_K^2}\left(L + \frac{1}{32\pi^2}\ln\frac{M_i^2}{\mu^2}\right) \tag{C.1}$$

[#10] Here we pick the renormalization point at $\mu_K = M_K$ for the kaon wave function renormalization. For $\pi$ and $\eta$, we take $M_\pi$ and $M_\eta$ in the tree-order Lagrangian as physical masses. This physical scheme is independent of the arbitrary mass scale $\mu_{\rm d.r.}$ figuring in the dimensional regularization.

where $L$ contains the divergence, and

$$\begin{aligned}
\alpha_s &= -\frac{1}{M_K^2}\left(-\frac{3}{4}\bar{h} + (l_1 - 2l_2 + l_3)(\hat{m} + m_s)\right) \\
\beta_s &= -\frac{1}{2}\left((g_2 - 2g_3 + g_6) + (g_4 - 2g_5 + g_7) + (g_8 - 2g_9)\right) \\
\alpha_v &= -\frac{1}{M_K^2}\left(-\frac{1}{4}\bar{h} + (l_1 + l_3)(\hat{m} + m_s)\right) \\
\beta_v &= -\frac{1}{2}\left((g_2 + g_6) + (g_4 + g_7) + g_8\right)
\end{aligned} \tag{C.2}$$

with

$$\bar{h} = h_1\hat{m} + h_2 m_s + h_3(2\hat{m} + m_s). \tag{C.3}$$

Here we have separated $\alpha_{s,v}$ and $\beta_{s,v}$ because in off-shell amplitudes, the constant $\alpha_{s,v}$ is multiplied by $\omega$ while the $\beta_{s,v}$ is multiplied by $\omega^3$, thus behaving differently for $\omega \neq M_K$. The constants $\gamma_{s,v}$ – coming from finite loop terms – and $\delta^{s,v}$ – multiplying the divergence – are given by

$$\begin{aligned}
\gamma_s &= -3M_K^2 - \frac{9}{4}M_K f_\pi(-M_K) - \frac{9}{4}M_K f_\eta(-M_K) - \frac{9}{4}(D+F)^2 M_\pi^2 \\
&\quad -\frac{1}{4}(D-3F)^2 M_\eta^2 + \left(\frac{3}{2}(D-F)^2 + \frac{1}{6}(D+3F)^2\right) M_K^2 \\
&\quad +|C|^2\left(\left(1+\sqrt{3}\right)C_\pi(-\delta_T) + \frac{1}{3\sqrt{3}}C_K(-\delta_T) - \frac{1}{4}F_K(-\delta_T)\right) \\
\gamma_v &= \frac{1}{3}M_\pi^2 - \frac{4}{3}M_K^2 + \frac{1}{4}M_K f_\pi(-M_K) - \frac{3}{4}M_K f_\eta(-M_K) + \frac{11}{12}(D+F)^2 M_\pi^2 \\
&\quad -\frac{1}{12}(D-3F)^2 M_\eta^2 + \left(-\frac{7}{6}(D-F)^2 + \frac{1}{18}(D+3F)^2\right) M_K^2 \\
&\quad +|C|^2\left(\left(1+\frac{1}{3\sqrt{3}}\right)C_\pi(-\delta_T) + \frac{1}{\sqrt{3}}C_K(-\delta_T) + \frac{2}{9}F_\pi(-\delta_T) + \frac{1}{36}F_K(-\delta_T)\right) \\
\delta_s^\pi &= \frac{9}{4}M_K^2 - \frac{3}{4}M_\pi^2 - \frac{27}{8}(D+F)^2 M_\pi^2 + |C|^2\left(3+3\sqrt{3}\right)(2\delta_T^2 - M_\pi^2) \\
\delta_s^K &= -\frac{3}{2}M_K^2 - \left(\frac{27}{8}(D-F)^2 + \frac{3}{8}(D+3F)^2\right) M_K^2 + |C|^2\left(\frac{3}{4} + \frac{1}{2\sqrt{3}}\right)(2\delta_T^2 - M_K^2) \\
\delta_s^\eta &= \frac{9}{4}M_K^2 - \frac{3}{4}M_\eta^2 - \frac{3}{8}(D-3F)^2 M_\eta^2 \\
\delta_v^\pi &= -\frac{1}{4}M_K^2 - \frac{1}{4}M_\pi^2 - \frac{9}{8}(D+F)^2 M_\pi^2 + |C|^2\left(\frac{5}{3} + \frac{1}{\sqrt{3}}\right)(2\delta_T^2 - M_\pi^2) \\
\delta_v^K &= \frac{1}{2}M_K^2 - \left(\frac{9}{8}(D-F)^2 + \frac{1}{8}(D+3F)^2\right) M_K^2 + |C|^2\left(-\frac{1}{12} + \frac{\sqrt{3}}{2}\right)(2\delta_T^2 - M_K^2) \\
\delta_v^\eta &= \frac{3}{4}M_K^2 - \frac{1}{4}M_\eta^2 - \frac{1}{8}(D-3F)^2 M_\eta^2
\end{aligned} \tag{C.4}$$

where $C_i(-\delta_T), F_i(-\delta_T)$ and $f_i(\omega)$ are

$$\begin{aligned}
C_i(-\delta_T) &= -(M_i^2 + \delta_T^2) - 3\delta_T f_i(-\delta_T) \\
F_i(-\delta_T) &= -\frac{4}{3}M_i^2 + 6\delta_T^2 + 6\delta_T f_i(-\delta_T)
\end{aligned}$$

$$f_i(\omega) = \sqrt{\omega^2 - M_i^2}\ln\left|\frac{\omega+\sqrt{\omega^2-M_i^2}}{\omega-\sqrt{\omega^2-M_i^2}}\right| \quad \text{for } \omega^2 > M_i^2$$
$$= \sqrt{M_i^2-\omega^2}\left(\pi + 2\sin^{-1}\frac{\omega}{M_i}\right) \quad \text{for } \omega^2 < M_i^2. \tag{C.5}$$

Note that $f_i(\omega)$ result from diagram of Fig. 1e as explained in Appendix A. We write the counter terms as

$$\alpha_{s,v} = \alpha^r_{s,v} + \alpha^{div}_{s,v}, \qquad \beta_{s,v} = \beta^r_{s,v} + \beta^{div}_{s,v} \tag{C.6}$$

where the divergent parts $\alpha^{div}_{s,v}$ and $\beta^{div}_{s,v}$ are to cancel the divergence part $L$ in eq.(C.1) and the finite counter terms $\alpha^r$ and $\beta^r$ are to be fixed by experiments. After removing the divergences, the constant $\bar{g}_{s,v}$ can be written as

$$\bar{g}_{s,v} = \alpha^r_{s,v} + \beta^r_{s,v} + \frac{1}{32\pi^2}\frac{1}{f^2M_K^2}\left(\gamma_{s,v} + \sum_{i=\pi,K,\eta}\delta^i_{s,v}\ln\frac{M_i^2}{\mu^2}\right). \tag{C.7}$$

Note that $\bar{g}_{s,v}$ is $\mu$-independent and hence can be fixed from experiments independently of $\mu$. How to do this for off-shell amplitudes is described in the main text.

## Appendix D: $1/m_B$ Corrections

In writing down the off-shell amplitudes with the parameters determined on-shell, we have assumed that the $\mathcal{O}(Q^2)$ terms quadratic in $\omega$ can be calculated by saturating the Born graphs with the octet and decuplet intermediate states. In calculating the decuplet contributions in the lowest order in $1/m_B$ from the Feynman graphs in relativistic formulation, one encounters the usual off-shell non-uniqueness characterized by a factor Z in the decuplet-nucleon-meson vertex when the decuplet is off-shell:

$$\mathcal{L} = C\bar{T}_\mu\left(g^{\mu\nu} - \left(Z+\frac{1}{2}\right)\gamma^\mu\gamma^\nu\right)A_\nu B + h.c.\ . \tag{D.1}$$

This gives the $Z$ dependence in the $1/m_B$ corrections to $\bar{d}_{s,v}$:

$$\bar{d}_{s,\frac{1}{m}} = -\frac{1}{48}\left((D+3F)^2+9(D-F)^2\right)\frac{1}{m_B} - \frac{1}{12}|C|^2\frac{1}{m_B}\left(Z+\frac{5}{2}\right)\left(\frac{1}{2}-Z\right)$$
$$\bar{d}_{v,\frac{1}{m}} = -\frac{1}{48}\left((D+3F)^2-3(D-F)^2\right)\frac{1}{m_B} + \frac{1}{36}|C|^2\frac{1}{m_B}\left(Z+\frac{5}{2}\right)\left(\frac{1}{2}-Z\right). \tag{D.2}$$

We shall fix $Z$ from $\pi N$ scattering ignoring $SU(3)$ breaking which occurs at higher chiral order than we need. The precise value of $Z$ turns out not to be important for both kaonic atoms and kaon condensation. Now our chiral Lagrangian gives, at tree order, the isoscalar $\pi N$ scattering length

$$a^{(+)}_{\pi N} = \frac{1}{4\pi f^2(1+M_\pi/m_B)}(2\tilde{D}_{\pi N}M_\pi^2 + \Sigma_{\pi N}) \tag{D.3}$$

where $\Sigma_{\pi N}$ is the $\pi N$ sigma term ($\approx 45MeV$) and $\tilde{D}_{\pi N} = \frac{1}{4}(d_1+d_2)+\frac{1}{2}(d_5+d_6)$. If we take the empirical value of $a^{(+)}_{\pi N} = -0.01M_\pi^{-1}$, we obtain

$$\tilde{D}^{emp}_{\pi N} \approx -1.29/m_B \approx -0.27 \text{ fm}. \tag{D.4}$$

The $1/m$ correction to $\pi N$ scattering is

$$\tilde{D}^{\frac{1}{m}}_{\pi N} = -\frac{(D+F)^2}{16}\frac{1}{m_B} - \frac{2}{9}|C|^2\frac{1}{m_B}\left(Z+\frac{5}{2}\right)\left(\frac{1}{2}-Z\right). \tag{D.5}$$

For the constants $D$, $F$ and $C$ used in this paper, this formula reproduces the experimental value (D.4) for $Z \simeq -0.5$. This will be used in our calculation of the off-shell amplitudes.

Alternatively one could fix $Z$ at one-loop order as in [27]. This however affects our results insignificantly. To see this, take $Z \approx 0.15$ obtained in ref.[27]. The resulting off-shell $KN$ amplitudes are given by the dotted lines in Fig.2. This represents less than 1 % change in the kaon self-energy, an uncertainty that can be safely ignored in the noise of other uncertainties inherent in heavy-baryon chiral perturbation theory.

## Appendix E: Off-Shell Amplitudes

In terms of the low-energy parameters fixed by the on-shell constraints, the off-shell $K^-N$ scattering amplitude is given by

$$\begin{aligned}
a^{K^-p} &= \frac{1}{4\pi(1+\omega/m_B)}\Big\{ T_v^{K^-p}(\omega=M_K) - \frac{\omega^2}{f^2}\left(\frac{\bar{g}^2_{\Lambda^\star{}_R}}{\omega+m_B-m_{\Lambda^\star{}_R}}\right) \\
&\quad +\frac{1}{f^2}(\omega-M_K)+\frac{1}{f^2}(\omega^2-M_K^2)\left(\bar{d}_s-\frac{\sigma_{KN}}{M_K^2}+\bar{d}_v+\frac{(\hat{m}+m_s)a_1}{2M_K^2}\right) \\
&\quad +\frac{1}{f^2}(L_p^+(\omega)-L_p^+(M_K))-\frac{1}{f^2}(L_p^-(\omega)-L_p^-(M_K))\Big\}, \qquad \text{(E.1)} \\
a^{K^-n} &= \frac{1}{4\pi(1+\omega/m_B)}\Big\{ T_v^{K^-n}(\omega=M_K) \\
&\quad \frac{1}{2f^2}(\omega-M_K)+\frac{1}{f^2}(\omega^2-M_K^2)\left(\bar{d}_s-\frac{\sigma_{KN}}{M_K^2}-\bar{d}_v-\frac{(\hat{m}+m_s)a_1}{2M_K^2}\right) \\
&\quad +\frac{1}{f^2}(L_n^+(\omega)-L_n^+(M_K))-\frac{1}{f^2}(L_n^-(\omega)-L_n^-(M_K))\Big\}. \qquad \text{(E.2)}
\end{aligned}$$

Here

$$\begin{aligned}
L_p^+(\omega) &= \frac{\omega^2}{64\pi f^2}\Big\{\Big[2(D-F)^2+\frac{1}{3}(D+3F)^2\Big]M_K+\frac{3}{2}(D+F)^2M_\pi \\
&\quad +\frac{1}{2}(D-3F)^2M_\eta-\frac{1}{3}(D+F)(D-3F)(M_\pi+M_\eta) \\
&\quad -\frac{1}{6}(D+F)(D-3F)(M_\pi^2+M_\eta^2)\int_0^1 dx\frac{1}{\sqrt{(1-x)M_\pi^2+xM_\eta^2}}\Big\} \\
&\quad +\frac{\omega^2}{8f^2}\left(4\Sigma_K^{(+)}(-\omega)+5\Sigma_K^{(+)}(\omega)+2\Sigma_\pi^{(+)}(\omega)+3\Sigma_\eta^{(+)}(\omega)\right), \\
L_p^-(\omega) &= \alpha_p M_K^2\omega+\beta_p\omega^3+\frac{1}{4f^2}\omega^2\left\{-\frac{1}{2}\Sigma_K^{(-)}(\omega)-\Sigma_\pi^{(-)}(\omega)-\frac{3}{2}\Sigma_\eta^{(-)}(\omega)\right\}, \\
L_p^-(M_K) &= (\bar{g}_s+\bar{g}_v)M_K^3, \\
L_n^+(\omega) &= \frac{1}{64\pi f^2}\omega^2\Big\{\Big[\frac{5}{2}(D-F)^2+\frac{1}{6}(D+3F)^2\Big]M_K+\frac{3}{2}(D+F)^2M_\pi
\end{aligned}$$

$$
\begin{aligned}
&+\frac{1}{2}(D-3F)^2 M_\eta + \frac{1}{3}(D+F)(D-3F)(M_\pi + M_\eta) \\
&+\frac{1}{6}(D+F)(D-3F)(M_\pi^2 + M_\eta^2)\int_0^1 dx \frac{1}{\sqrt{(1-x)M_\pi^2 + xM_\eta^2}}\Big\} \\
&+\frac{\omega^2}{8f^2}\cdot\left(2\Sigma_K^{(+)}(-\omega) + \Sigma_K^{(+)}(\omega) + \frac{5}{2}\Sigma_\pi^{(+)}(\omega) + \frac{3}{2}\Sigma_\eta^{(+)}(\omega)\right), \\
L_n^-(\omega) &= \alpha_n M_K^2 \omega + \beta_n \omega^3 + \frac{1}{4f^2}\omega^2\left\{\frac{1}{2}\Sigma_K^{(-)}(\omega) - \frac{5}{4}\Sigma_\pi^{(-)}(\omega) - \frac{3}{4}\Sigma_\eta^{(-)}(\omega)\right\}, \\
L_n^-(M_K) &= (\bar{g}_s - \bar{g}_v)M_K^3,
\end{aligned}
\tag{E.3}
$$

where

$$
\begin{aligned}
\Sigma_i^{(+)}(\omega) &= -\frac{1}{4\pi}\sqrt{M_i^2 - \omega^2}\times\theta(M_i - |\omega|) + \frac{i}{2\pi}\sqrt{\omega^2 - M_i^2}\times\theta(\omega - M_i), \\
\Sigma_i^{(-)}(\omega) &= -\frac{1}{4\pi^2}\sqrt{\omega^2 - M_i^2}\ln\left|\frac{\omega + \sqrt{\omega^2 - M_i^2}}{\omega - \sqrt{\omega^2 - M_i^2}}\right|\times\theta(|\omega| - M_i) \\
&\quad -\frac{1}{2\pi^2}\sqrt{M_i^2 - \omega^2}\sin^{-1}\frac{\omega}{M_i}\times\theta(M_i - |\omega|).
\end{aligned}
\tag{E.4}
$$

Note that $\Sigma_i^{\pm}(\omega)$ result from diagrams of Fig. 1e (See Appendix A), where intermediate states can be real particle and result in imaginary amplitude. The functions $L_{p,n}^-(\omega)$ contain four parameters $\alpha_{p,n}$ and $\beta_{p,n}$. Owing to the constraints at $\omega = M_K$, $L_{p,n}^-(M_K)$, they reduce to two. These two cannot be fixed by on-shell data. However since the off-shell amplitudes are rather insensitive to the precise values of these constants, we will somewhat arbitrarily set $\alpha_{p,n} \approx \beta_{p,n}$ in calculating Figure 2.

## Appendix F: Interpolating Fields

In this Appendix, we show explicitly that to the chiral order we are concerned with, physics does not depend on the way the kaon field $K$ (or in general the Goldstone boson field $\pi$) interpolates. There is nothing new in what we do below: It is a well-known theorem [#11]. But to those who are not very familiar with the modern notion of effective field theories, it has been a bit of a mystery that an off-shell amplitude which does not obey Adler's soft-pion theorem such as in the case of our Lagrangian could give the same physics with the amplitude which does in a situation which involves the equation of state, not just an on-shell S-matrix. To have a simple idea, we start with the toy model of Manohar [#12].

**• Adler's Conditions in a Toy Model**

Consider the simple Lagrangian,

$$
\mathcal{L} = \frac{1}{2}(\partial K)^2 - \frac{1}{2}M_K^2(1 + \epsilon\bar{B}B)K^2 \tag{F.1}
$$

[#11] A general discussion closely related to this issue is given in a recent paper by Leutwyler [41].

[#12] We wish to thank A. Manohar who showed us how to understand the problem using this toy model.

where $K$ is the charged kaon field which will develop a condensate in the form $\langle K^- \rangle = v_K e^{-i\mu t}$. As written, this Lagrangian can give only a linear density dependence in the kaon self-energy at tree order. The effective energy-density for s-wave kaon condensation linear in $v_K^2$ is

$$\tilde{\epsilon} \;=\; (\mu^2 - M_K^2(1+\epsilon\rho_N))v_K^2. \tag{F.2}$$

Thus the chemical potential in the ground state is

$$\mu^2 = M_K^2(1+\epsilon\rho_N). \tag{F.3}$$

We shall now redefine the kaon field. To do this, we have, from the Noether construction and the equation of motion,

$$\begin{aligned} j_A^\mu &= f\partial^\mu K, \\ \partial_\mu j_A^\mu &= f M_K^2(1+\epsilon\bar{B}B)K. \end{aligned} \tag{F.4}$$

This invites us to redefine the kaon field as

$$\tilde{K} = K(1+\epsilon\bar{B}B) = \frac{\partial_\mu j_A^\mu}{f M_K^2} \tag{F.5}$$

thus giving the divergence of the axial current as the interpolating field of the kaon field. This kaon field will then satisfy the Adler soft-meson theorem. To see this, we rewrite the original Lagrangian in terms of the new field $\tilde{K}$,

$$\begin{aligned} \mathcal{L} &= \frac{1}{(1+\epsilon\bar{B}B)^2}\left(\frac{1}{2}\left(\partial\tilde{K}\right)^2 - \frac{1}{2}M_K^2(1+\epsilon\bar{B}B)\tilde{K}^2\right) + \mathcal{O}(\partial B) \\ &= \frac{1}{2}(1-2\epsilon\bar{B}B)\left(\partial\tilde{K}\right)^2 - \frac{1}{2}M_K^2(1-\epsilon\bar{B}B)\tilde{K}^2 + \mathcal{O}\left(\tilde{K}^2(\bar{B}B)^{n\geq 2}\right) + \mathcal{O}(\partial B). \end{aligned} \tag{F.6}$$

We can immediately read off the $KN$ scattering amplitude and verify that it satisfies the Adler theorem. Note, however, that to obtain the same kaon self-energy that enters into the energy-density of the matter system as the one given by eq.(F.1), it would be necessary to keep multi-baryon terms, which means that in medium, higher density dependence needs to be taken into account.

Now to see that the interpolating fields $K$ and $\bar{K}$ give the same physics in medium, consider the critical point at which condensation sets in. From eq.(F.5), we have

$$|\langle\tilde{K}\rangle| \;=\; \tilde{v}_K = v_K(1+\epsilon\rho_N). \tag{F.7}$$

Substituting this into eq.(F.1) or directly from eq.(F.6), we get the effective energy-density

$$\tilde{\epsilon} \;=\; (\mu^2 - M_K^2(1+\epsilon\rho_N))\frac{\tilde{v}_K^2}{(1+\epsilon\rho_N)^2}. \tag{F.8}$$

Clearly (F.2) and (F.8) give the same critical point given by the vanishing of the energy density. This is of course quite trivial. If one keeps terms up to linear in $\rho_N$, eq.(F.8) reads

$$\tilde{\epsilon} \;=\; (\mu^2 - M_K^2 - (2\mu^2 - M_K^2)\epsilon\rho_N)\tilde{v}_K^2. \tag{F.9}$$

This is the kaon self-energy in linear density approximation, which satisfies Adler's consistency condition. As it stands, it looks very different from eq.(F.2), but to the linear order in density, this gives the same pole position,

$$\begin{aligned}(\mu^2 - M_K^2 - (2\mu^2 - M_K^2)\epsilon\rho_N) = 0 \quad &\longrightarrow \quad (1 - 2\epsilon\rho_N)\mu^2 = M_K^2(1 - \epsilon\rho_N) \\ &\longrightarrow \quad \mu^2 = M_K^2(1 + \epsilon\rho_N). \end{aligned} \tag{F.10}$$

Beyond the linear-density approximation, one must use eq.(F.8) instead of eq.(F.9) for the physics of the toy-model Lagrangian: Consistency requires that *all* kaon-multi-nucleon scattering terms (that is, terms higher order in $\rho_N$) be included.

We now turn to the real issue. We shall compare the approach used here (called "Kaplan-Nelson" (KN)) to the Gasser-Sainio-Svarc (GSS) approach which implements Adler's conditions by means of external fields [30].

**• The KN Approach**

The KN approach corresponds to introducing the source field $p_i$ in the Lagrangian

$$\mathcal{L}_{source} \;=\; p^+K^- + p^-K^+ \cdots . \tag{F.11}$$

The self-energy is then obtained from

$$\begin{aligned}\langle\tau(x_1,x_2)\rangle &= \langle T(K^+(x_2)K^-(x_1))\rangle_\rho \\ &= -\left\langle \frac{\delta^2}{\delta p^+(x_1)\delta p^-(x_2)} \int \mathcal{D}[K,B] e^{i\int(\mathcal{L}_{orig}+\mathcal{L}_{source})}\Big|_{p^\pm=0,\cdots=0}\right\rangle_\rho \\ &= i\Delta_K^{(0)}(x_1-x_2) + i\Sigma_K \int \Delta_K^{(0)}(x_1-z)\Delta_K^{(0)}(z-x_2) + \mathcal{O}(\Sigma_K^2) \end{aligned} \tag{F.12}$$

where $\langle\cdots\rangle_\rho$ represents the expectation value in the ground state of dense matter. Here $\Delta_K^{(0)}$ is the free kaon propagator

$$\Delta_K^{(0)}(x-y) = \frac{1}{(2\pi)^4}\int \frac{e^{-ik\cdot(x-y)}}{k^2 - M_K^2 + i\epsilon} d^4k \tag{F.13}$$

and $\Sigma_K$ is the kaon self-energy calculated to order $\nu = 3$ with the Lagrangian

$$\begin{aligned}\mathcal{L}_0 &= \partial K^+ \partial K^- - M_K^2 K^+K^- \\ \mathcal{L}_{int} &= \mathcal{L}_{int}^{\nu=1} + \mathcal{L}_{int}^{\nu=2} + \cdots . \end{aligned} \tag{F.14}$$

Summing the series (F.12), we have

$$\tau(x_1,x_2) \;=\; \frac{i}{(2\pi)^4}\int \frac{e^{ik\cdot(x_1-x_2)}}{k^2 - M_K^2 - \Sigma_K + i\epsilon} d^4k. \tag{F.15}$$

The propagator to order $\nu = 3$ in momentum space is

$$\Delta_K \;=\; \frac{i}{k^2 - M_K^2 - \Sigma_K + i\epsilon} \tag{F.16}$$

and the effective energy density to order $v_K^2$ is

$$\begin{aligned}\epsilon &= -i\Delta_K^{-1}|v_K|^2 \\ &= -(\mu^2 - M_K^2 - \Sigma_K)|v_K|^2. \end{aligned} \tag{F.17}$$

**• The GSS Approach**

The GSS approach corresponds to introducing into the Lagrangian the source field $p_i$ of the form

$$\mathcal{L}_{source} = p^+K^-(1+\alpha_p\bar{p}p+\alpha_n\bar{n}n)+p^-K^+(1+\alpha_p\bar{p}p+\alpha_n\bar{n}n)+\cdots \tag{F.18}$$

where $\alpha_p = \frac{1}{f^2M_K^2}(\sigma_{KN}+C_{KN})$ and $\alpha_n = \frac{1}{f^2M_K^2}(\sigma_{KN}-C_{KN})$ are related with the parameters of the Lagrangian (2) by

$$\sigma_{KN} = -\frac{1}{2}(\hat{m}+m_s)(a_1+2a_2+4a_3)$$

and

$$C_{KN} = -\frac{1}{2}(\hat{m}+m_s)a_1.$$

As shown in ref.[30], this way of introducing the source field reproduces Adler's conditions (soft-pion, self-consistency etc.). Now the self-energy is obtained from the two-point function

$$\begin{aligned}\langle\tau(x_1,x_2)\rangle &= -\left\langle \frac{\delta^2}{\delta p^+(x_1)\delta p^-(x_2)}\int \mathcal{D}[K,B]e^{i\int(\mathcal{L}_{orig}+\mathcal{L}_{source})}\right|_{p^\pm=0,\cdots=0}\Bigg\rangle_\rho \\ &= \langle T(K^+(1+\alpha_p\bar{p}p+\alpha_n\bar{n}n)(x_2)K^-(1+\alpha_p\bar{p}p+\alpha_n\bar{n}n)(x_1)\rangle_\rho \\ &= (1+\alpha_p\rho_p+\alpha_n\rho_n)^2\langle T(K^+(x_2)K^-(x_1))\rangle_\rho \\ &= (1+\alpha_p\rho_p+\alpha_n\rho_n)^2\frac{i}{(2\pi)^4}\int\frac{e^{ik\cdot(x_1-x_2)}}{k^2-M_K^2-\Sigma_K+i\epsilon}d^4k \end{aligned} \tag{F.19}$$

where $\Sigma_K$ is identical to that of the KN approach since the $\alpha_p$ and $\alpha_n$ are $\nu=2$ terms that are unaffected by loop corrections (of order $\nu=3$). Finally the full propagator is given by

$$\Delta'_K = (1+\alpha_p\rho_p+\alpha_n\rho_n)^2\frac{i}{k^2-M_K^2-\Sigma_K+i\epsilon} \tag{F.20}$$

which can be rewritten in the form of eq.(F.16);

$$\Delta'_K = \frac{i}{k^2-M_K^2-\Sigma'_K+i\epsilon} \tag{F.21}$$

with a redefined self-energy

$$\Sigma'_K = \frac{1}{(1+\alpha_p\rho_p+\alpha_n\rho_n)^2}\left\{(k^2-M_K^2)\left[(1+\alpha_p\rho_p+\alpha_n\rho_n)^2-1\right]+\Sigma_K\right\}. \tag{F.22}$$

One can verify that to the linear order in density, this has the structure mentioned in the main text, namely, it changes from an attraction on-shell to a repulsion off-shell. Finally the effective energy density linear in $\tilde{v}_K^2$ is

$$\tilde{\epsilon} = -i(\Delta'_K)^{-1}|\tilde{v}_K|^2 = -i\Delta_K^{-1}\left|\frac{\tilde{v}_K}{1+\alpha_p\rho_p+\alpha_n\rho_n}\right|^2 \tag{F.23}$$

where $\tilde{v}_K$ is the kaon expectation value in terms of the GSS field.

**• Effective energy-density and physical observables**

As in the toy model, we can write $\tilde{v}_K$ in terms of $v_K$:

$$\tilde{v}_K = v_K(1+ax+b) \tag{F.24}$$

where $a=(\alpha_p-\alpha_n)\rho$ and $b=\alpha_n\rho$. Thus the energy-densities to all orders in $v_K$ and $\tilde{v}_K$ can be written as

$$\epsilon = \sum_{n\geq 2}\alpha_n(\mu,x,\rho)|v_K|^n+\beta(\mu,x,\rho), \tag{F.25}$$

$$\tilde{\epsilon} = \sum_{n\geq 2}\alpha_n(\mu,x,\rho)\left|\frac{\tilde{v}_K}{1+ax+b}\right|^n+\beta(\mu,x,\rho) \tag{F.26}$$

where $a_n(\mu,x,\rho)$ and $\beta(\mu,x,\rho)$ are given in eq.(37). By differentiating the effective energy density with respect to $\mu,x,v_K$ ($\tilde{v}_K$), one can get the equation of state as a function of density $\rho$. In the GSS approach, we have three equations of state;

$$\begin{aligned}
0=\frac{\partial\tilde{\epsilon}}{\partial\mu} &= \sum_{n\geq 2}\frac{\partial\alpha_n(\mu,x,\rho)}{\partial\mu}\left(\frac{\tilde{v}_K}{1+ax+b}\right)^n+\frac{\partial\beta(\mu,x,\rho)}{\partial\mu}\\
0=\frac{\partial\tilde{\epsilon}}{\partial x} &= \sum_{n\geq 2}\frac{\partial\alpha_n(\mu,x,\rho)}{\partial x}\left(\frac{\tilde{v}_K}{1+ax+b}\right)^n+\frac{\partial\beta(\mu,x,\rho)}{\partial x}\\
&\quad +\frac{a}{1+ax+b}\sum_{n\geq 2}n\alpha_n(\mu,x,\rho)\left(\frac{\tilde{v}_K}{1+ax+b}\right)^n\\
0=\frac{\partial\epsilon}{\partial\tilde{v}_K} &= \frac{1}{\tilde{v}_K}\sum_{n\geq 2}n\alpha_n(\mu,x,\rho)\left(\frac{\tilde{v}_K}{1+ax+b}\right)^n.
\end{aligned} \tag{F.27}$$

Now using the third equation, we see that the last term in the second equation vanishes. To see that the two ways give the same physics, it suffices to note that the KN approach gives the same set of equations except for the replacement $\tilde{v}_K=v_K(1+ax+b)$ which does not affect anything.

An identical conclusion is reached by Thorsson and Wirzba [42] by a slightly different reasoning.

# Appendix G: In-Medium Modifications

In this Appendix we write down the explicit forms of the quantities that enter in eq.(28).

$$\begin{aligned}
\delta\mathcal{T}^{K^-p}_{\rho_N} &= -\frac{1}{12f^4}\Big\{(D+F)^2\left[(M_\pi^2+M_K^2-\omega^2)D^n_{4,\pi\pi}-D^n_{6,\pi\pi}\right]\\
&\quad +\frac{1}{2}(D+F)^2\left[(M_\pi^2+M_K^2-\omega^2)D^p_{4,\pi\pi}-D^p_{6,\pi\pi}\right]\\
&\quad +\frac{1}{2}(D-3F)^2\left[\left(M_K^2-\frac{1}{3}M_\pi^2-\omega^2\right)D^p_{4,\eta\eta}-D^p_{6,\eta\eta}\right]\\
&\quad -(D+F)(D-3F)\left[\left(\frac{1}{3}M_\pi^2-\frac{1}{3}M_K^2-\omega^2\right)D^p_{4,\pi\eta}-D^p_{6,\pi\eta}\right]\Big\}
\end{aligned}$$

$$
\begin{aligned}
&+\frac{\omega^2}{4f^4}\left(8\Sigma_K^p(\omega)+\Sigma_K^n(\omega)\right)+\frac{1}{12f^4}\Big\{2(D+F)FM_\pi^2\Sigma_\pi^p(0)\\
&+(D+F)^2M_\pi^2\Sigma_\pi^n(0)-2(D-3F)FM_\eta^2\Sigma_\eta^p(0)\Big\} \qquad \text{(G.1)}\\
\delta\mathcal{T}_{\rho_N}^{K^-n} &= -\frac{1}{12f^4}\Big\{(D+F)^2\left[(M_\pi^2+M_K^2-\omega^2)D_{4,\pi\pi}^p-D_{6,\pi\pi}^p\right]\\
&+\frac{1}{2}(D+F)^2\left[(M_\pi^2+M_K^2-\omega^2)D_{4,\pi\pi}^n-D_{6,\pi\pi}^n\right]\\
&+\frac{1}{2}(D-3F)^2\left[\left(M_K^2-\frac{1}{3}M_\pi^2-\omega^2\right)D_{4,\eta\eta}^n-D_{6,\eta\eta}^n\right]\\
&+(D+F)(D-3F)\left[\left(\frac{1}{3}M_\pi^2-\frac{1}{3}M_K^2-\omega^2\right)D_{4,\pi\eta}^n-D_{6,\pi\eta}^n\right]\Big\}\\
&+\frac{\omega^2}{4f^4}\left(2\Sigma_K^n(\omega)+\Sigma_K^p(\omega)\right)+\frac{1}{12f^4}\Big\{(D^2-F^2)M_\pi^2\Sigma_\pi^n(0)\\
&+(D+F)^2M_\pi^2\Sigma_\pi^p(0)+(D-3F)(D-F)M_\eta^2\Sigma_\eta^n(0)\Big\}, \qquad \text{(G.2)}\\
D_{\alpha,ij}^N &= \frac{1}{2\pi^2}\int_0^{k_{F_N}}d|\vec{k}|\frac{1}{|\vec{k}|^2+M_i^2}\frac{1}{|\vec{k}|^2+M_j^2}|\vec{k}|^\alpha\\
\Sigma_i^N(\omega) &= \frac{1}{2\pi^2}\int_0^{k_{F_N}}d|\vec{k}|\frac{|\vec{k}|^2}{\omega^2-M_i^2-|\vec{k}|^2}. \qquad \text{(G.3)}
\end{aligned}
$$

Here the subscripts $\pi$, $\eta$ and $K$ are the octet Goldstone bosons, the superscripts $n$ and $p$ stand for neutrons and protons.

## References


[1] G. E. Brown, C.-H. Lee, M. Rho and V. Thorsson, Nucl. Phys. **A567** (1994) 937.

[2] C.-H. Lee, H. Jung, D.-P. Min and M. Rho, Phys. Lett. **B326** (1994) 14.

[3] C.-H. Lee, G. E. Brown and M. Rho, SNUTP-94-28, hep-ph/9403339.

[4] G.E. Brown and H.A. Bethe, Astrophys. Jour. 423 (1994) 659.

[5] D. B. Kaplan and A. E. Nelson, Phys. Lett. **B175** (1986) 57.

[6] G.E. Brown, K. Kubodera and M. Rho, Phys. Lett. **B192** (1987) 273.

[7] H. D. Politzer and M. B. Wise, Phys. Lett. **B273** (1991) 156.

[8] G. E. Brown, K. Kubodera, M. Rho and V. Thorsson, Phys. Lett. **B 291** (1992) 355.

[9] V. Thorsson, M. Prakash and J. Lattimer, Nucl. Rhys. **A572** (1994) 693.

[10] H. Yabu, S. Nakamura, F. Myhrer and K. Kubodera, Phys. Lett. **B315** (1993) 17.

[11] M. Lutz, A. Steiner and W. Weise, "Kaons in dense matter", to be published.

[12] S. Weinberg, Phys. Lett. **B251** (1990) 288; Nucl. Phys. **B363** (1991) 3.

[13] C. Ordóñez, L. Ray and U. van Kolck, Phys. Rev. Lett. **72** (1994) 1982.

[14] M. Rho, Phys. Rev. Lett. **66** (1991) 1275.

[15] T.-S. Park, D.-P. Min and M. Rho, Phys. Repts. **233** (1993) 341.

[16] T.-S. Park, I.S. Towner and K. Kubodera, to be published.

[17] E. Jenkins and A. Manohar, Phys. Lett. **B255** (1991) 558; E. Jenkins and A. Manohar, Phys. Lett. **B259** (1991) 353; E. Jenkins, Nucl. Phys. **B368** (1992) 190; E. Jenkins *et al.*, UCSD/PTH 92-34.

[18] E. Friedman, A. Gal and C.J. Batty, Phys. Lett. **B308** (1993) 6; A. Gal, private communication to G.E. Brown.

[19] C.G. Callan and I. Klebanov, NP**B 262** (1985) 365; C.G. Callan, K. Hornbostel and I. Klebanov, PL**B 202** (1988) 269; N.N. Scoccola, D.-P. Min, H. Nadeau and M. Rho, Nucl. Phys. **A505** (1989) 497.

[20] D. Montano, H. D. Politzer and M.B. Wise, Nucl. Phys. **B375** (1992) 507.

[21] A. Steiner and W. Weise, to be published.

[22] T. Barnes and E.S. Swanson, Phys. Rev. **C49** (1994) 1166.

[23] O. Dumbrais et al, Nucl. Phys. **B216** (1982) 277; G.C. Oades, talk given at the NORDITA Workshop on Mesons in Nuclei and Kaon Condensation, 25-27 April 1994.

[24] P.B. Siegel and W. Weise, Phys. Rev. **C38** (1988) 221; A. Müller-Groeling, K. Holinde and J. Speth, Nucl. Phys. **A513** (1990) 557.

[25] M.J. Savage, CMU-HEP 94-11, NSF-ITP-94-33.

[26] N.N. Scoccola, private communication to M. Rho.

[27] V. Bernard, N. Kaiser and U.-G. Meissner, Phys. Lett. **B 309** (1993) 421.

[28] S.L. Adler and R.F. Dashen, *Current Algebra and Applications to Particle Physics* (Benjamin, New York, 1968).

[29] C. Callan, S. Coleman, J. Wess and B. Zumino, Phys. Rev. **177** (1969) 2247.

[30] J. Gasser, M.E. Sainio and A. Svarc, Nucl. Phys. **B307** (1988) 779.

[31] J. Stachel, Nucl. Phys. **A566** (1994) 183c.

[32] G.E. Brown and M. Rho, "Chiral restoration in hot and/or dense matter," to appear.

[33] G. Baym, Phys. Rev. Lett. **30** (1973) 1340.

[34] M. Prakash, T.L. Ainsworth and J.M. Lattimer, Phys. Rev. Lett. **61** (1988) 2518.

[35] M. Rho, Phys. Repts. **240** (1994) 1.

[36] G.E. Brown and M. Rho, Phys. Rev. Lett. **66** (1991) 2720.

[37] C.J. Pethick and D.G. Ravenhall, Ann. Phys. (NY) **183** (1988) 131.

[38] J.B. Kogut, D.K. Sinclair and K.C. Wang, Phys. Lett. **B 263** (1991) 101.

[39] R. Shankar, Reviews of Modern Phys. **66** (1994) 129; J. Polchinski, in *Recent Directions in Particle Physics* ed. by J. Harvey and J. Polchinski (World Scientific, Singapore, 1993) p 235.

[40] H.K. Lee, M. Rho and S.J. Sin, work in progress.

[41] H. Leutwyler, "On the foundations of chiral perturbation theory," BUTP-93/24.

[42] V. Thorsson, Talk given at the 1993 Chiral Symmetry Workshop at ECT*, September, 1993, Trento, Italy; A. Wirzba, Talk given at the NORDITA Workshop on Mesons in Nuclei and Kaon Condensation, April 25-17, 1994, Copenhagen, Denmark; V. Thorsson and A. Wirzba, to appear.

Table 1 : Scattering lengths from three leading order contributions for the empirical value of the constant $g^2_{\Lambda^\star} = 0.25$. Also shown is the contribution from $\Lambda^\star$.

| $g^2_{\Lambda^\star} = 0.25$ | $\mathcal{O}(Q)$ | $\mathcal{O}(Q^2)$ | $\mathcal{O}(Q^3)$ | $\Lambda^\star$ |
|---|---|---|---|---|
| $a^{K^+p}(fm)$ | $-0.588$ | 0.316 | $-0.114$ | 0.076 |
| $a^{K^-p}(fm)$ | 0.588 | 0.316 | $-0.143$ | $-1.431$ |
| $a^{K^+n}(fm)$ | $-0.294$ | 0.277 | $-0.183$ | 0.000 |
| $a^{K^-n}(fm)$ | 0.294 | 0.277 | $-0.201$ | 0.000 |

Table 2 :Self energies for kaonic atoms in nuclear matter ($x = 0.5$) in unit of $M_K^2$ at $u = 0.97$ for $g^2_{\Lambda^\star} = 0.25$. $\Delta V = M_K^* - M_K$ is the attraction (in unit of MeV) at a given $(C^S_{\Lambda^\star} - C^T_{\Lambda^\star})f^2$.

| $(C^S_{\Lambda^\star} - C^T_{\Lambda^\star})f^2$ | $M_K^*$ | $\Delta V$ | $-\rho\mathcal{T}^{free}$ | $-\rho\delta\mathcal{T}^{free}$ | $\Pi^1_{\Lambda^\star}$ | $\Pi^2_{\Lambda^\star}$ |
|---|---|---|---|---|---|---|
| 1 | 396.4 | $-98.65$ | $-0.2361$ | 0.04485 | $-0.2113$ | 0.04344 |
| 5 | 351.4 | $-143.6$ | $-0.1810$ | 0.03111 | $-0.3541$ | 0.00903 |
| 10 | 326.2 | $-168.8$ | $-0.1738$ | 0.02637 | $-0.4215$ | 0.00418 |
| 50 | 253.9 | $-241.1$ | $-0.1842$ | 0.01839 | $-0.5715$ | 0.00056 |
| 100 | 218.7 | $-276.3$ | $-0.1927$ | 0.01621 | $-0.6281$ | 0.00021 |

Table 3 :Self-energies for kaonic atoms in nuclear matter ($x = 0.5$) in unit of $M_K^2$ for $g^2_{\Lambda^\star} = 0.25$ and $(C^S_{\Lambda^\star} - C^T_{\Lambda^\star})f^2 = 10$. $\Delta V \equiv M_K^\star - M_K$ is the attraction (in unit of MeV) at given density.

| $u$ | $M_K^*$ | $\Delta V$ | $-\rho\mathcal{T}^{free}$ | $-\rho\delta\mathcal{T}^{free}$ | $\Pi^1_{\Lambda^\star}$ | $\Pi^2_{\Lambda^\star}$ |
|---|---|---|---|---|---|---|
| 0.2 | 424.6 | $-70.37$ | $-0.0673$ | 0.0034 | $-0.1998$ | 0.007607 |
| 0.4 | 390.0 | $-105.0$ | $-0.0920$ | 0.0084 | $-0.3024$ | 0.006641 |
| 0.6 | 364.3 | $-130.7$ | $-0.1173$ | 0.0143 | $-0.3610$ | 0.005635 |
| 0.8 | 342.6 | $-152.4$ | $-0.1462$ | 0.0207 | $-0.3996$ | 0.004794 |
| 1.0 | 323.5 | $-171.5$ | $-0.1789$ | 0.0274 | $-0.4250$ | 0.004088 |
| 1.2 | 306.2 | $-188.8$ | $-0.2150$ | 0.0343 | $-0.4404$ | 0.003483 |
| 1.4 | 289.9 | $-205.1$ | $-0.2540$ | 0.0413 | $-0.4460$ | 0.002945 |

Table 4 : Numerical values in MeV of $r$ as function of $x$ and $u$.

| $r(u,x)$ | $x=0.0$ | $x=0.5$ | $x=1.0$ |
|---|---|---|---|
| $u=0.5$ | 30.78 | 38.25 | 30.78 |
| $u=1.0$ | 47.52 | 61.55 | 47.52 |
| $u=1.5$ | 60.20 | 79.75 | 60.20 |

Table 5 : Self-energies for $K^+$ in nuclear matter ($x=0.5$) in unit of $M_K^2$ for $g_{\Lambda^\star}^2=0.25$ and $(C_{\Lambda^\star}^S - C_{\Lambda^\star}^T)f^2 = 10$. $\Delta V \equiv M_K^\star - M_K$ is the repulsion (in unit of MeV) at given density.

| $u$ | $M_K^*$ | $\Delta V$ | $-\rho\mathcal{T}^{free}$ | $-\rho\delta\mathcal{T}^{free}$ | $\Pi^1_{\Lambda^\star}$ | $\Pi^2_{\Lambda^\star}$ |
|---|---|---|---|---|---|---|
| 0.2 | 507 | 12 | 0.025 | 0.019 | $-0.0009$ | 0.0002 |
| 0.4 | 515 | 20 | 0.048 | 0.040 | $-0.0038$ | 0.0005 |
| 0.6 | 523 | 28 | 0.068 | 0.053 | $-0.0087$ | 0.0006 |
| 0.8 | 532 | 37 | 0.085 | 0.054 | $-0.0157$ | 0.0006 |
| 1.0 | 537 | 42 | 0.102 | 0.083 | $-0.0248$ | 0.0010 |
| 1.2 | 542 | 47 | 0.117 | 0.112 | $-0.0360$ | 0.0014 |
| 1.4 | 547 | 52 | 0.129 | 0.122 | $-0.0494$ | 0.0015 |

Table 6 : Critical density $u_c$ in in-medium two-loop chiral perturbation theory for $g_{\Lambda^\star}^2 = 0.25$. (a) correspond to linear density approximation of Fig .3a and (b) to the full two-loop result for $(C_{\Lambda^\star}^S - C_{\Lambda^\star}^T)f^2 = 10$.

| | | $(b)$ | | |
|---|---|---|---|---|
| $F(u)$ | $(a)$ | $C_{\Lambda^\star}^S f^2 = 10$ | $C_{\Lambda^\star}^S f^2 = 5$ | $C_{\Lambda^\star}^S f^2 = 0$ |
| $\frac{2u^2}{1+u}$ | 3.77 | 2.81 | 2.98 | 3.24 |
| $u$ | 3.90 | 3.13 | 3.33 | 3.69 |
| $\sqrt{u}$ | 4.11 | 3.71 | 3.96 | 4.41 |

Table 7 : Critical density $u_c$ in in-medium two-loop chiral perturbation theory for $g^2_{\Lambda^\star} = 0.25$ and $F(u) = u$.

| $(C^S_{\Lambda^\star} - C^T_{\Lambda^\star})f^2$ | $C^S_{\Lambda^\star} f^2 = 100$ | $C^S_{\Lambda^\star} f^2 = 10$ | $C^S_{\Lambda^\star} f^2 = 0$ |
|---|---|---|---|
| 1 | 2.25 | 3.25 | 4.51 |
| 10 | 2.24 | 3.13 | 3.69 |
| 100 | 2.18 | 2.66 | 2.77 |

Table 8 :Self-energies for kaonic atoms in nuclear matter ($x = 0.5$) in unit of $M^2_K$ at $u = 0.97$ for $g^2_{\Lambda^\star} = 0.05$. $\Delta V = M^*_K - M_K$ is the attraction (in unit of MeV) at a given $(C^S_{\Lambda^\star} - C^T_{\Lambda^\star})f^2$.

| $(C^S_{\Lambda^\star} - C^T_{\Lambda^\star})f^2$ | $M^*_K$ | $\Delta V$ | $-\rho\mathcal{T}^{free}$ | $-\rho\delta\mathcal{T}^{free}$ | $\Pi^1_{\Lambda^\star}$ | $\Pi^2_{\Lambda^\star}$ |
|---|---|---|---|---|---|---|
| 10 | 386 | −109 | −0.114 | 0.0407 | −0.3187 | 0.001164 |
| 20 | 364 | −131 | −0.116 | 0.0342 | −0.3773 | 0.000548 |
| 50 | 330 | −165 | −0.128 | 0.0270 | −0.4535 | 0.000187 |
| 70 | 316 | −179 | −0.135 | 0.0248 | −0.4822 | 0.000123 |
| 100 | 300 | −195 | −0.143 | 0.0227 | −0.5129 | 0.000079 |

Table 9 : Critical density $u_c$ in in-medium two-loop ChPT for $(C^S_{\Lambda^\star} - C^T_{\Lambda^\star})f^2 = 70$, $g^2_{\Lambda^\star} = 0.05$.

| $F(u)$ | $C^S_{\Lambda^\star} f^2 = 70$ | $C^S_{\Lambda^\star} f^2 = 40$ | $C^S_{\Lambda^\star} f^2 = 10$ | $C^S_{\Lambda^\star} f^2 = 0$ |
|---|---|---|---|---|
| $\frac{2u^2}{1+u}$ | 2.68 | 2.83 | 3.04 | 3.14 |
| $u$ | 2.99 | 3.17 | 3.45 | 3.59 |
| $\sqrt{u}$ | 3.56 | 3.79 | 4.15 | 4.35 |

Table 10 : Critical density $u_c$ in in-medium two-loop ChPT for $g^2_{\Lambda^\star} = 0.05$ and $F(u) = u$.

| $(C_{\Lambda^\star} - C^T_{\Lambda^\star})f^2$ | $C^S_{\Lambda^\star} f^2 = 100$ | $C^S_{\Lambda^\star} f^2 = 10$ | $C^S_{\Lambda^\star} f^2 = 0$ |
|---|---|---|---|
| 1 | 2.95 | 4.07 | 5.34(?) |
| 10 | 2.94 | 3.91 | 4.44 |
| 100 | 2.83 | 3.33 | 3.44 |

Table 11 :Self-energies for kaonic atoms *with BR scaling* in nuclear matter ($x = 0.5$) in unit of $M^2_K$ at $u = 0.97$ for $g^2_{\Lambda^\star} = 0.25$. $\Delta V = M^*_K - M_K$ is the attraction (in unit of MeV) at a given $(C^S_{\Lambda^\star} - C^T_{\Lambda^\star})f^2$.

| $(C^S_{\Lambda^\star} - C^T_{\Lambda^\star})f^2$ | $M^*_K$ | $\Delta V$ | $-\rho\mathcal{T}^{free}$ | $-\rho\delta\mathcal{T}^{free}$ | $\Pi^1_{\Lambda^\star}$ | $\Pi^2_{\Lambda^\star}$ |
|---|---|---|---|---|---|---|
| 1 | 386.5 | −108.5 | −0.2985 | 0.04102 | −0.1626 | 0.02995 |
| 5 | 344.5 | −150.5 | −0.2596 | 0.02966 | −0.3056 | 0.00727 |
| 10 | 319.5 | −175.5 | −0.2550 | 0.02533 | −0.3698 | 0.00343 |
| 50 | 246.3 | −248.7 | −0.2677 | 0.01786 | −0.5026 | 0.00045 |
| 100 | 211.7 | −283.3 | −0.2759 | 0.01585 | −0.5565 | 0.00017 |

Table 12 :Self-energies for kaonic atoms *with BR scaling* in nuclear matter ($x = 0.5$) in unit of $M^2_K$ for $g^2_{\Lambda^\star} = 0.25$ and $(C^S_{\Lambda^\star} - C^T_{\Lambda^\star})f^2 = 10$. $\Delta V \equiv M^\star_K - M_K$ is the attraction (in unit of MeV) at given density.

| $u$ | $M^*_K$ | $\Delta V$ | $-\rho\mathcal{T}^{free}$ | $-\rho\delta\mathcal{T}^{free}$ | $\Pi^1_{\Lambda^\star}$ | $\Pi^2_{\Lambda^\star}$ |
|---|---|---|---|---|---|---|
| 0.2 | 424.2 | −70.75 | −0.0698 | 0.00340 | −0.1977 | 0.00749 |
| 0.4 | 389.0 | −106.0 | −0.1032 | 0.00834 | −0.2946 | 0.00639 |
| 0.6 | 361.9 | −133.1 | −0.1445 | 0.01405 | −0.3421 | 0.00521 |
| 0.8 | 338.3 | −156.7 | −0.1982 | 0.02011 | −0.3655 | 0.00420 |
| 1.0 | 316.2 | −178.8 | −0.2661 | 0.02625 | −0.3691 | 0.00331 |
| 1.2 | 294.7 | −200.3 | −0.3498 | 0.03228 | −0.3569 | 0.00253 |
| 1.4 | 272.7 | −222.3 | −0.4511 | 0.03798 | −0.3291 | 0.00184 |

Table 13 : Critical density $u_c$ *with BR scaling* in in-medium two-loop chiral perturbation theory for $g^2_{\Lambda^\star} = 0.25$. (a) correspond to linear density approximation of Fig .3a and (b) to the full two-loop result for $(C^S_{\Lambda^\star} - C^T_{\Lambda^\star})f^2 = 10$.

| | | $(b)$ | | |
|---|---|---|---|---|
| $F(u)$ | $(a)$ | $C^S_{\Lambda^\star} f^2 = 10$ | $C^S_{\Lambda^\star} f^2 = 5$ | $C^S_{\Lambda^\star} f^2 = 0$ |
| $\frac{2u^2}{1+u}$ | 2.11 | 2.08 | 2.11 | 2.14 |
| $u$ | 2.16 | 2.15 | 2.17 | 2.20 |
| $\sqrt{u}$ | 2.22 | 2.23 | 2.25 | 2.26 |

Table 14 : Critical density $u_c$ *with BR scaling* in in-medium two-loop chiral perturbation theory for $g^2_{\Lambda^\star} = 0.25$ and $F(u) = u$.

| $(C^S_{\Lambda^\star} - C^T_{\Lambda^\star})f^2$ | $C^S_{\Lambda^\star} f^2 = 100$ | $C^S_{\Lambda^\star} f^2 = 10$ | $C^S_{\Lambda^\star} f^2 = 0$ |
|---|---|---|---|
| 1 | 1.92 | 2.16 | 2.21 |
| 10 | 1.92 | 2.15 | 2.20 |
| 100 | 1.89 | 2.09 | 2.12 |

Table 15 : Critical density $u_c$ *with BR scaling* and without $\mathcal{O}(Q^3)$ terms for (A) $C^S_{\Lambda^\star} = C^T_{\Lambda^\star} = 0$ and (B) $(C^S_{\Lambda^\star} - C^T_{\Lambda^\star})f^2 = 10$. This should be compared with the results of Table 13.

| | | $(B)$ | | |
|---|---|---|---|---|
| $F(u)$ | $(A)$ | $C^S_{\Lambda^\star} = 100$ | $C^S_{\Lambda^\star} = 10$ | $C^S_{\Lambda^\star} = 0$ |
| $\frac{2u^2}{1+u}$ | 1.89 | 1.68 | 1.85 | 1.88 |
| $u$ | 1.94(1.944) | 1.76 | 1.91 | 1.94(1.938) |
| $\sqrt{u}$ | 2.00(1.999) | 1.87 | 1.98 | 2.00(1.997) |

## Figure Captions

- **Figure 1:** One-loop Feynman diagrams contributing to $K^{\pm}N$ scattering: The solid line represents baryons (nucleon for the external and octet and decuplet baryons for the internal line) and the broken line pseudo-Goldstone bosons ($K^{\pm}$ for the external and $K$, $\pi$ and $\eta$ for the internal line). There are in total thirteen diagrams at one loop, but for s-wave $KN$ scattering, for reasons described in the text, we are left with only six topologically distinct one-loop diagrams.

- **Figure 2:** $K^-N$ amplitudes as function of $\sqrt{s}$: These figures correspond to eqs.(23) and (24) with $\bar{g}^2_{\Lambda^\star} = 0.25$, $\Gamma_{\Lambda^\star} = 50$ MeV and $\alpha_{p,n} = \beta_{p,n}$, fixed in the way described in the text. The first kink corresponds to the $KN$ threshold and the second around 1.5 GeV to $\sqrt{s} = m_B + M_\eta$ for $M_\eta \approx 547$ MeV. The solid line of $\mathcal{R}e$ part correspond to $Z = -0.5$ and the dashed line correspond to $Z = 0.15$, and the imaginary parts are independent of $Z$ value.

- **Figure 3:** (a): The linear density approximation to the kaon self-energy in medium, $\Pi_K$. The square blob represents the off-shell $K^-N$ amplitude calculated to $\mathcal{O}(Q^3)$; (b)-(f): medium corrections to $\mathcal{T}^{KN}$ of fig.(a) with the free nucleon propagator indicated by a double slash replaced by an in-medium one, eq.(24). The loop labeled $\rho_N$ represents the in-medium nucleon loop proportional to density, $N^{-1}$ the nucleon hole ($n^{-1}$ and/or $p^{-1}$), the external dotted line stands for the $K^-$ and the internal dotted line for the pseudoscalar octet $\pi$, $\eta$, $K$.

- **Figure 4:** Two-loop diagrams involving $\Lambda^\star$ contributing to the kaon self-energy. The diagrams (a) and (b) involve four-Fermi interactions, while the diagram (c) does not involve four-Fermi interactions and hence can be unambiguously determined by on-shell parameters. Here the internal dotted line represents the kaon.

- **Figure 5:** Plot of the $K^{\pm}$ effective potential in nuclear matter ($x = 0.5$). The upper solid line corresponds to $K^+$ "effective mass" without the *BR scaling*, and the lower solid (dashed) line to $K^-$ "effective mass" without (with) the *BR scaling*.

- **Figure 6:** One-loop diagrams contributing to the $\Lambda^\star$ mass shift in dense medium. The diagram (a) involves the intermediate states of $K^-p$ and $\bar{K}^0n$ and (b) the four-Fermi interaction $C^S_{\Lambda^\star}$ with both protons and neutrons.

- **Figure 7:** Plot of the proton fraction $x(u)$ prior to kaon condensation for different forms of $F(u)$.

- **Figure 8:** Plot of the quantity $M^\star_K$ obtained from the dispersion formula $D^{-1}(\mu, u) = 0$ vs. the chemical potential $\mu$ prior to kaon condensation for $g^2_{\Lambda^\star} = 0.25$ and $F(u) = 2u^2/(1+u)$. The solid line corresponds to the linear density approximation and the dashed lines to the in-medium two-loop results for $(C^S_{\Lambda^\star} - C^T_{\Lambda^\star})f^2 = 10$ and $C^S_{\Lambda^\star} f^2 = 10, 5, 0$ respectively from the left. The point at which the chemical potential $\mu$ intersects $M^\star_K$ corresponds to the critical point.

- **Figure 9:** The same as Figure 8 for $F(u) = u$.

- **Figure 10:** The same as Figure 8 for $F(u) = \sqrt{u}$.

- **Figure 11:** The same as Figure 8 with the *BR scaling* for $F(u) = 2u^2/(1+u)$.
- **Figure 12:** The same as Figure 8 with the *BR scaling* for $F(u) = u$.
- **Figure 13:** The same as Figure 8 with the *BR scaling* for $F(u) = \sqrt{u}$.

This figure "fig1-1.png" is available in "png"  format from:

http://arXiv.org/ps/hep-ph/9406311v2

This figure "fig2-1.png" is available in "png" format from:

http://arXiv.org/ps/hep-ph/9406311v2

This figure "fig3-1.png" is available in "png"  format from:

http://arXiv.org/ps/hep-ph/9406311v2

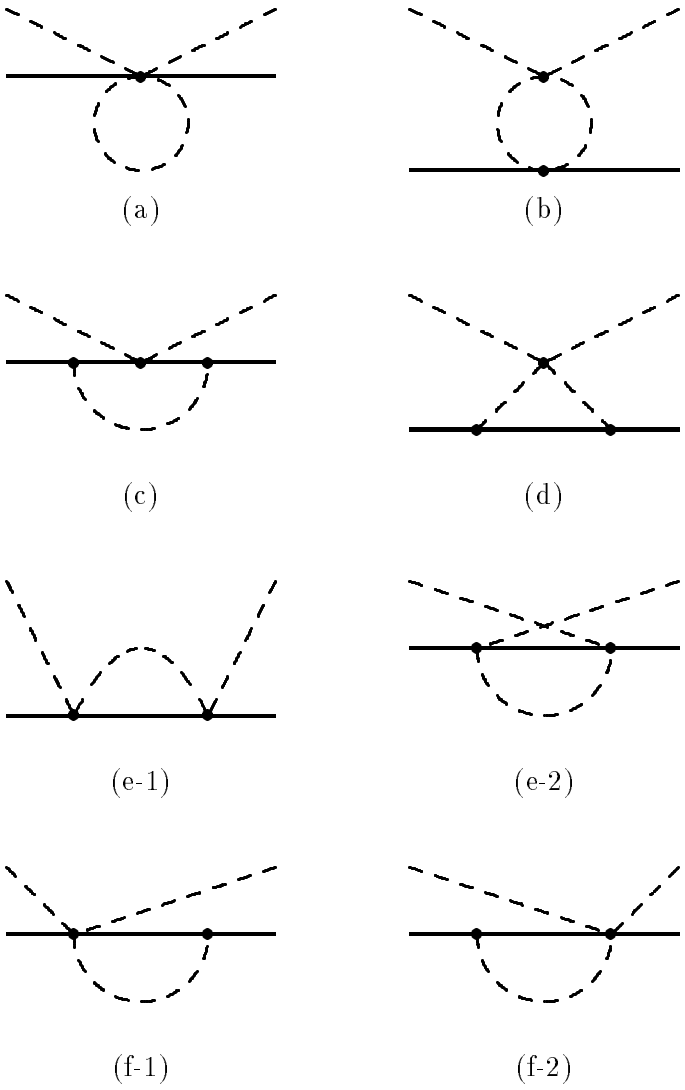


Figure 1

This figure "fig1-2.png" is available in "png" format from:

http://arXiv.org/ps/hep-ph/9406311v2

This figure "fig2-2.png" is available in "png" format from:

http://arXiv.org/ps/hep-ph/9406311v2

This figure "fig3-2.png" is available in "png" format from:

http://arXiv.org/ps/hep-ph/9406311v2

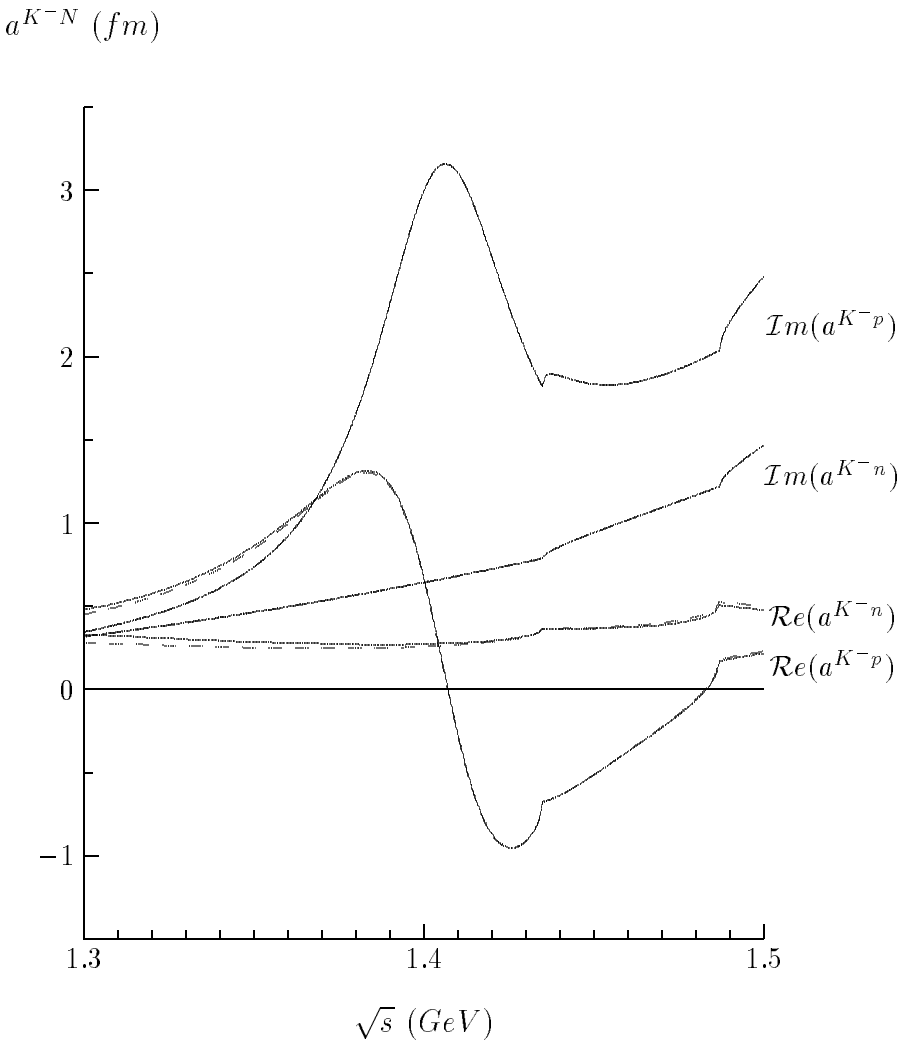
$a^{K^-N}\ (fm)$
3
2
1
0
−1
1.3
1.4
1.5
$\mathcal{I}m(a^{K^-p})$
$\mathcal{I}m(a^{K^-n})$
$\mathcal{R}e(a^{K^-n})$
$\mathcal{R}e(a^{K^-p})$
$\sqrt{s}\ (GeV)$

Figure 2

This figure "fig1-3.png" is available in "png"  format from:

http://arXiv.org/ps/hep-ph/9406311v2

This figure "fig2-3.png" is available in "png"  format from:

http://arXiv.org/ps/hep-ph/9406311v2

This figure "fig3-3.png" is available in "png"  format from:

http://arXiv.org/ps/hep-ph/9406311v2

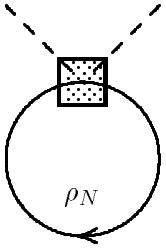


(a)

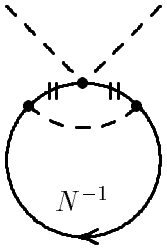


(b)

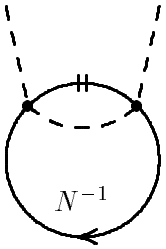


(c)

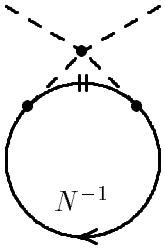


(d)

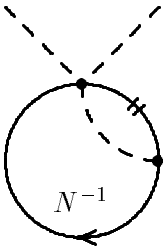


(e)

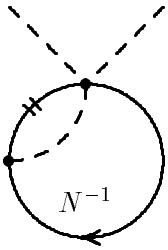


(f)

Figure 3

This figure "fig1-4.png" is available in "png"  format from:

http://arXiv.org/ps/hep-ph/9406311v2

This figure "fig2-4.png" is available in "png"  format from:

http://arXiv.org/ps/hep-ph/9406311v2

This figure "fig3-4.png" is available in "png" format from:

http://arXiv.org/ps/hep-ph/9406311v2

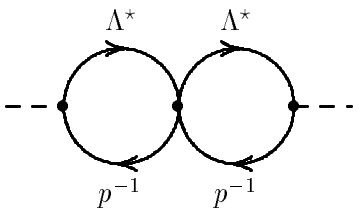
$\Lambda^\star$
$\Lambda^\star$
$p^{-1}$
$p^{-1}$

(a)

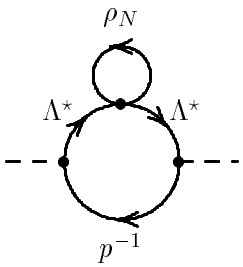
$\rho_N$
$\Lambda^\star$
$\Lambda^\star$
$p^{-1}$

(b)

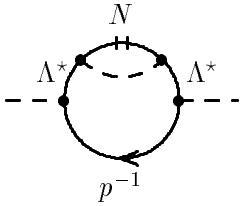
$N$
$\Lambda^\star$
$\Lambda^\star$
$p^{-1}$

(c)

Figure 4

This figure "fig1-5.png" is available in "png"  format from:

http://arXiv.org/ps/hep-ph/9406311v2

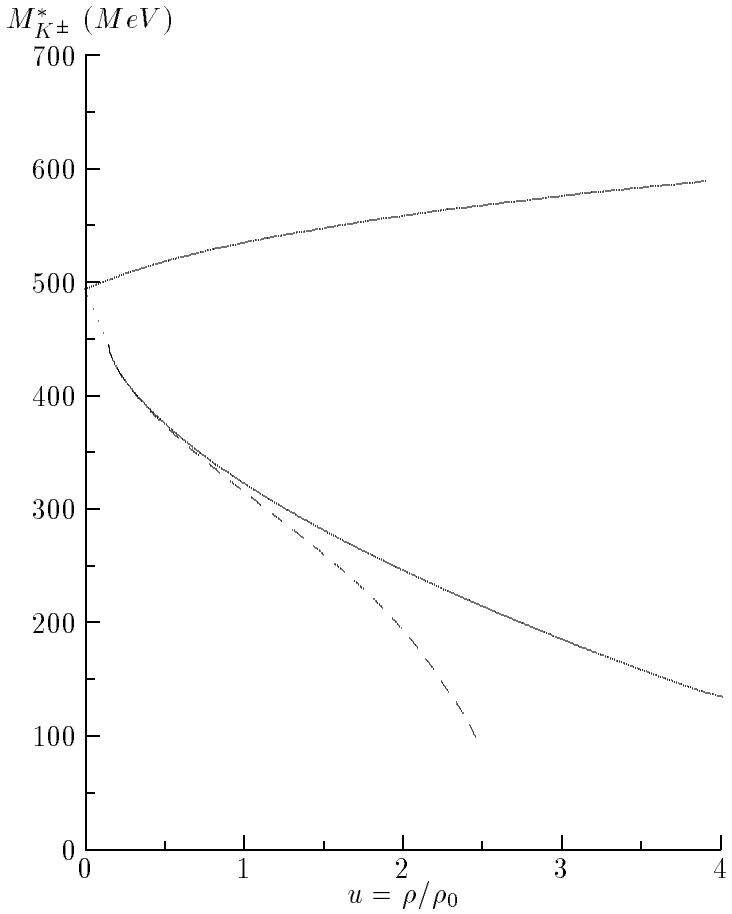


Figure 5

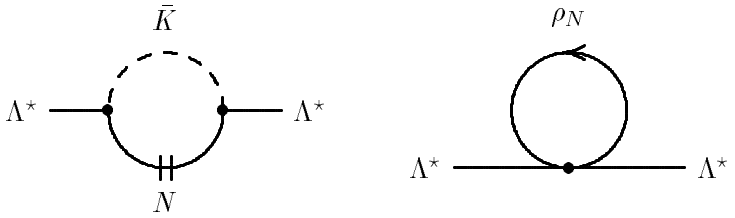


(a) (b)

Figure 6

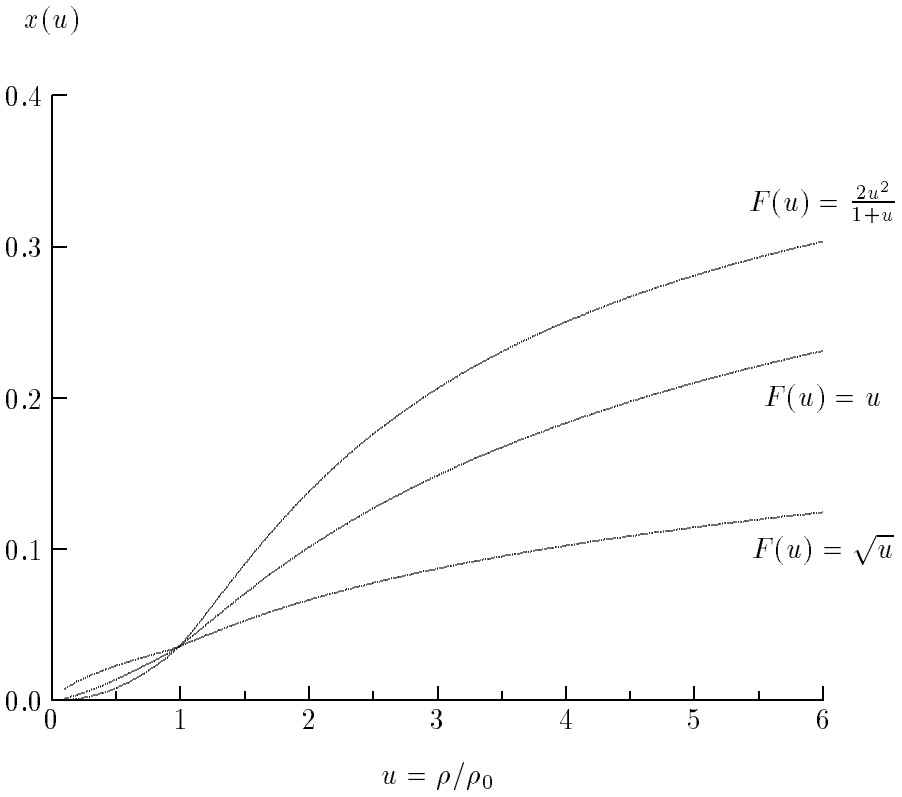


Figure 7

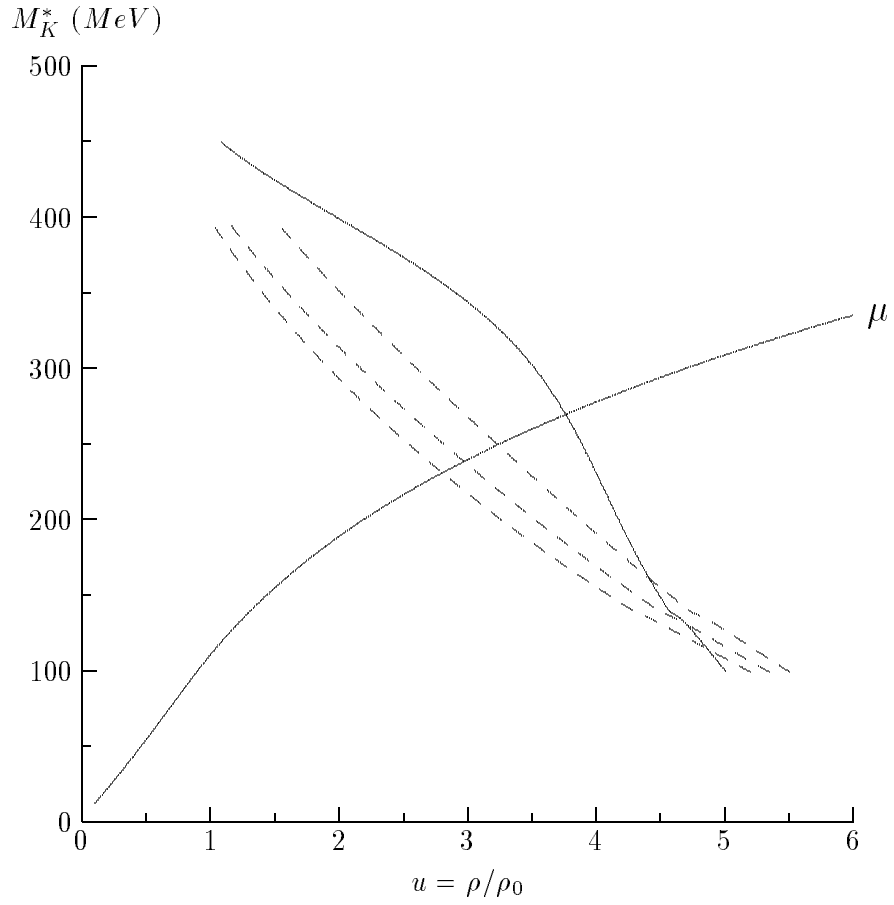


Figure 8

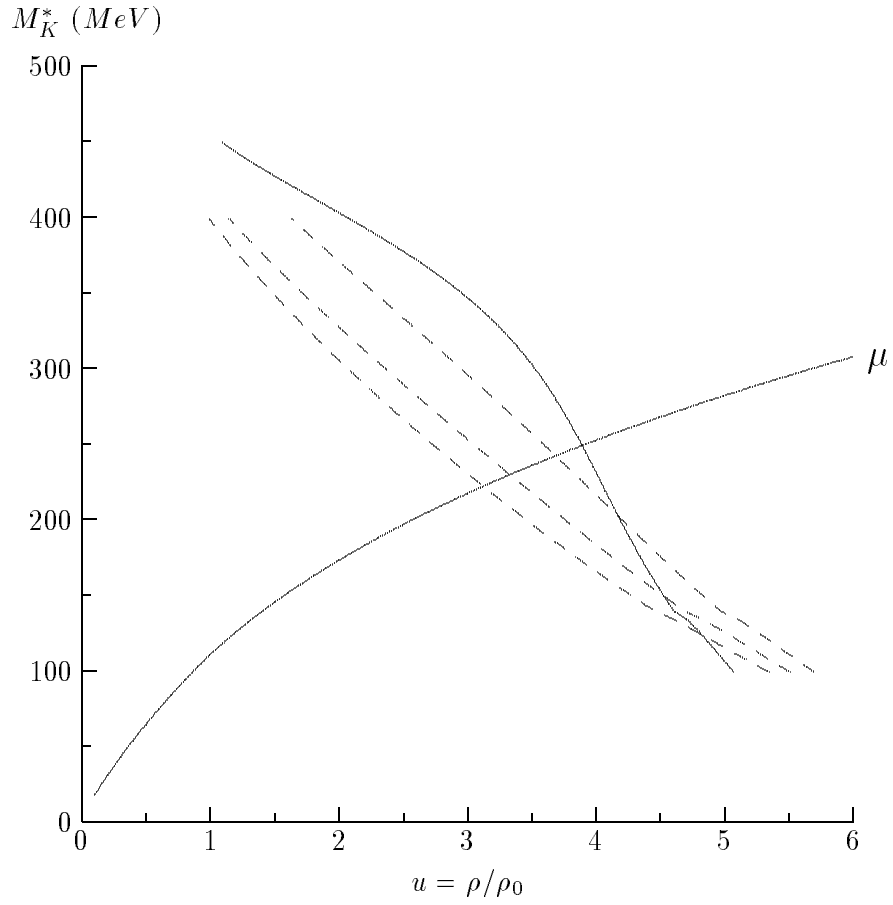


Figure 9

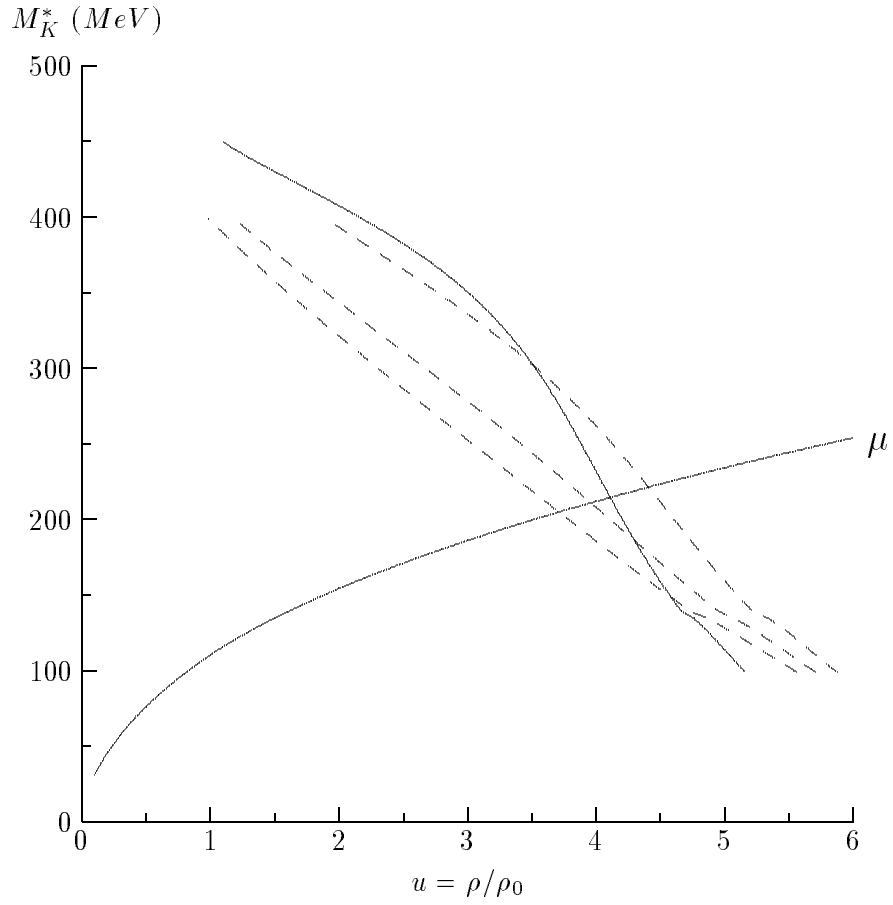


Figure 10

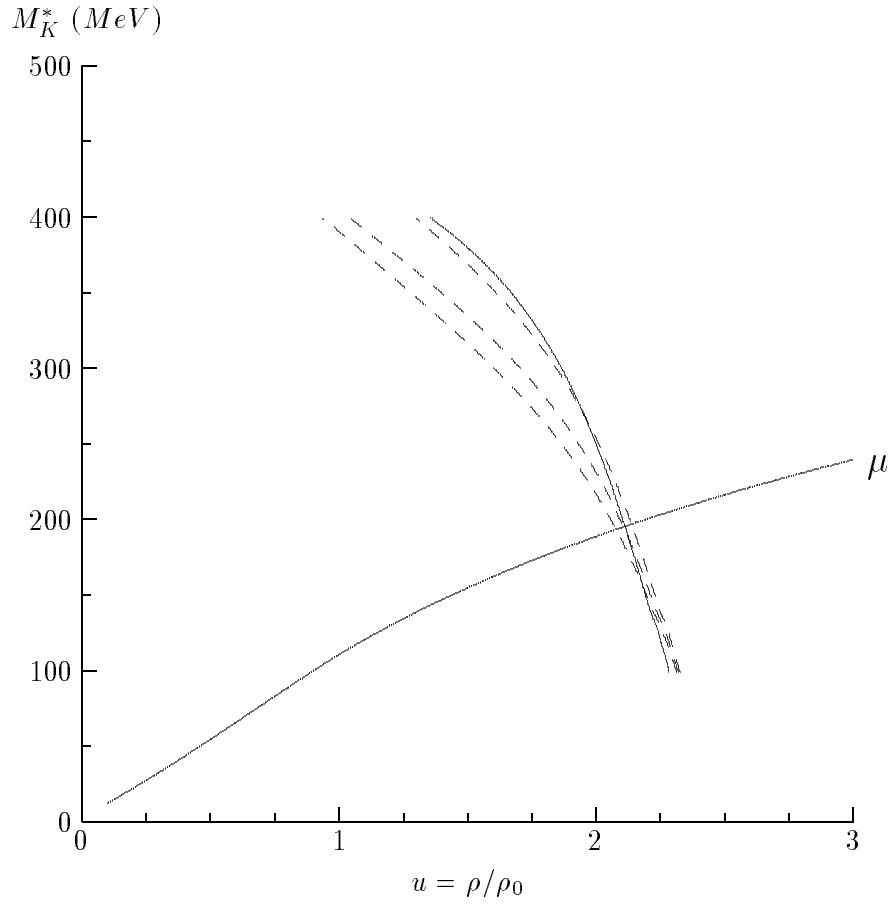


Figure 11

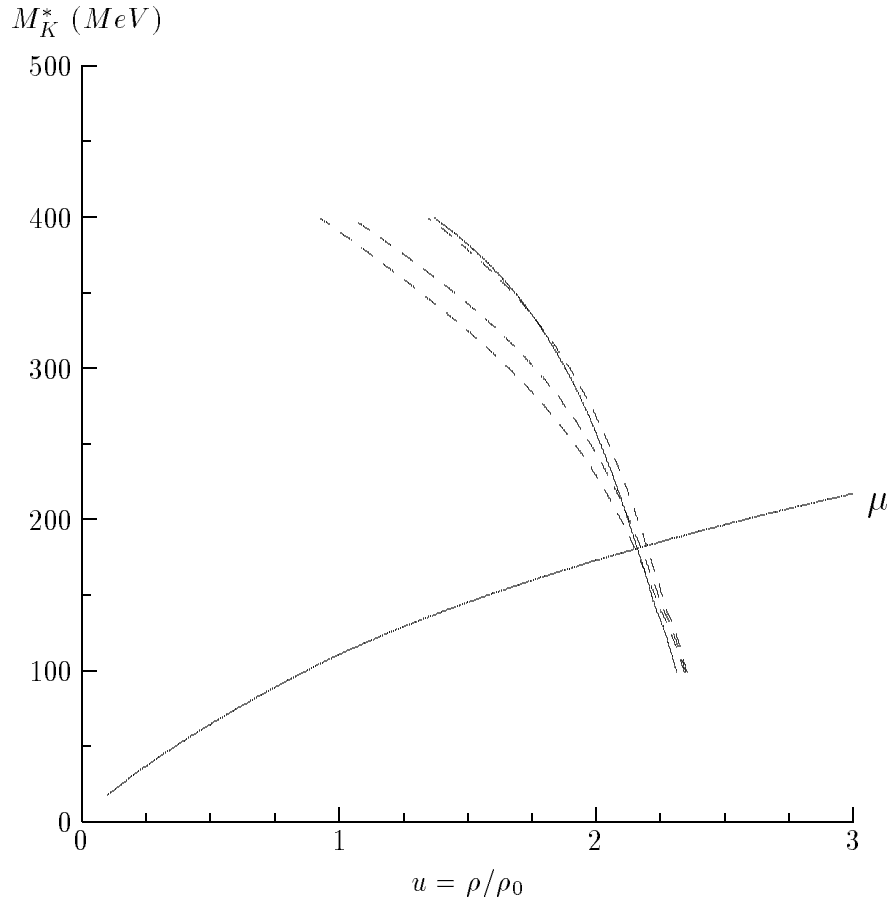


Figure 12

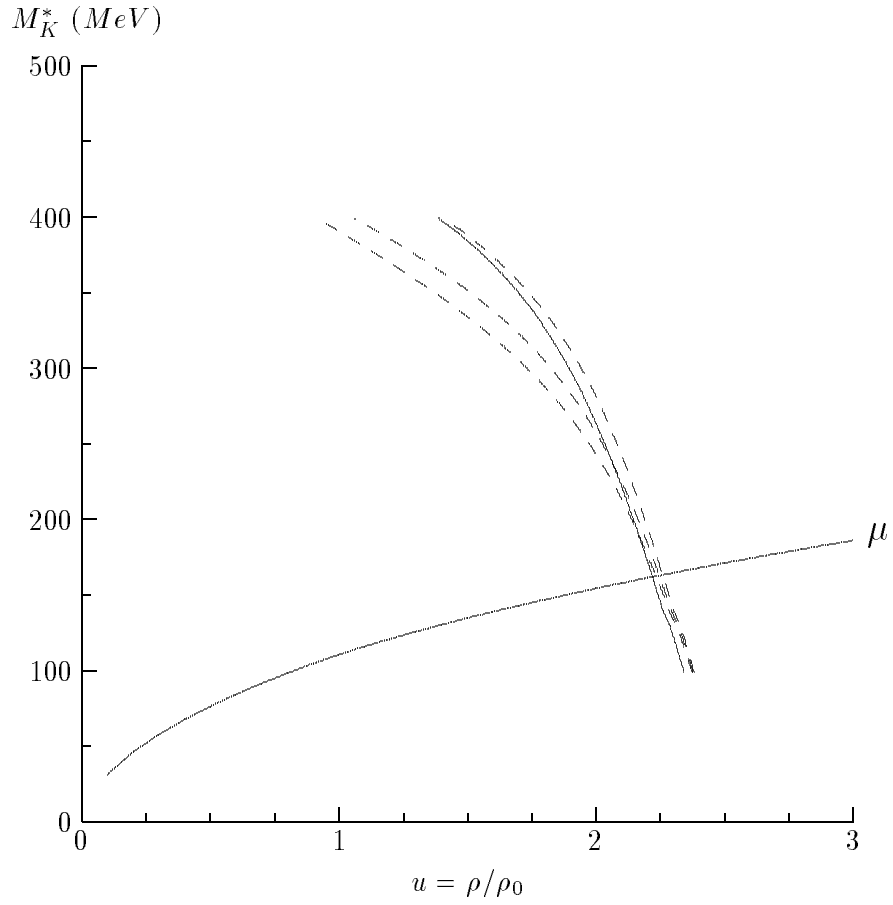


Figure 13